General Disclaimer

One or more of the Following Statements may affect this Document

- This document has been reproduced from the best copy furnished by the organizational source. It is being released in the interest of making available as much information as possible.

- This document may contain data, which exceeds the sheet parameters. It was furnished in this condition by the organizational source and is the best copy available.

- This document may contain tone-on-tone or color graphs, charts and/or pictures, which have been reproduced in black and white.

- This document is paginated as submitted by the original source.

- Portions of this document are not fully legible due to the historical nature of some of the material. However, it is the best reproduction available from the original submission.

Produced by the NASA Center for Aerospace Information (CASI)

(NASA-CR-150113) COMPARISON OF THE NONLINEAR DYNAMIC CHARACTERISTICS OF BARBER S-2 AND ASF RIDE CONTROL FREIGHT TRUCKS (Martin Marietta Corp.) 42 p HC A03/MF A01 CSCL 05H G3/54

N77-13655

Unclas 56967

MCR-76-475
Contract NAS 8-29882

Technical Report

September 1976

COMPARISON OF THE NONLINEAR DYNAMIC CHARACTERISTICS OF BARBER S-2 AND ASF RIDE CONTROL FREIGHT TRUCKS

Author:

P. Abbott

P. Abbott

Approved by:

G. Morosow

G. Morosow
Program Manager

DEC 1976
RECEIVED
NASA STI FACILITY
INPUT BRANCH

MARTIN MARIETTA CORPORATION
DENVER DIVISION
Denver, Colorado 80201

BARBER/ASF COMPARISON REPORT

Summary

This report presents the results of an experimental and analytical program to define the load deflection characteristics of a Barber S-2 freight truck and to compare these characteristics to those of an ASF freight truck of the same load capacity. The comparison of the two trucks is made on a parameter basis and on the basis of the wheel/rail loads induced by track misalignment.

The results of this study indicate there is very little difference in the parameters and the response of the two trucks. This is of course qualified by the assumptions required in the development of the mathematical models. It was hoped that field test data would be available for the verification of these assumptions. When this data does become available it will be included in our final Track Train Dynamics report.

Introduction

The purpose of this program was to experimentally define the parameters which may be used to describe the load/deflection characteristics of the Barber S-2 freight truck (70 ton capacity) for the significant modes of deformation of that truck. These parameters were then to be compared to those previously determined for an ASF ride control truck (70 ton capacity).

There has been a lot of attention devoted to this particular truck configuration due to the very low speeds at which the self-excited instability, called hunting, occurs. The analytical work of Cooperrider and Law has indicated that several degrees of freedom (or modes of deformation) are important in the determination of hunting speeds. These are:

1. bolster roll,
2. bolster lateral translation, and
3. truck warping (lozenging).

The experimental work performed in this program provides a set of parameters which describe the load/deformation characteristics of the degrees of freedom listed above.

The approach to the experimental determination of the parameters was identical to that taken on the test program of the ASF truck. Before getting into the test details let us discuss the actual parameters being considered and the physical behavior of the hardware.

The ASF and Barber trucks for the particular truck configuration - two axles, two side frames and one bolster - are practically identical in appearance. The connection between the bolster and side frame is made through a group of coil springs (vertically) and a friction device called a wedge. This connection is illustrated schematically below.

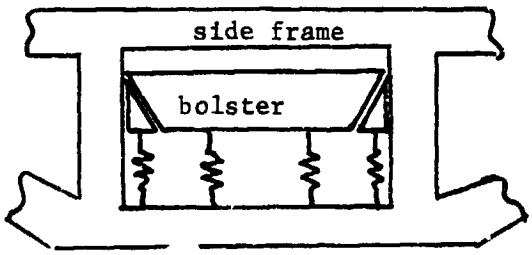

Barber design

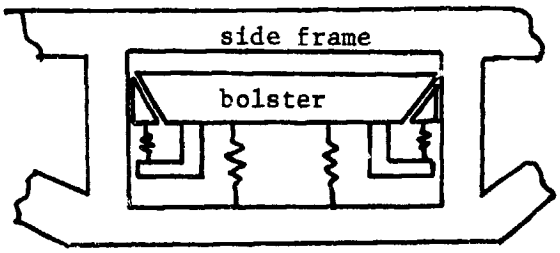

ASF design

The coil springs provide load paths both vertically and laterally for both the ASF and Barber designs. The friction wedges provide a Coulomb type friction force for vertical and lateral relative motions between the bolster and side frame. Roll, of course, is merely

differential vertical motion between the bolster and side frames. The Barber and ASF designs differ in the manner in which friction is controlled. The force Fv as shown in the previous sketch is constant for the ASF design and a function of relative vertical displacement between bolster and side frame for the Barber design.

The side frame/axle connection is essentially the same for the two designs, having a bearing adapter and roller bearing.

The structural elements themselves may be considered to be rigid for all practical purposes. The relative motions within the truck are the result of sliding and coil spring deformations.

A general "model" of this behavior may be represented as shown below.

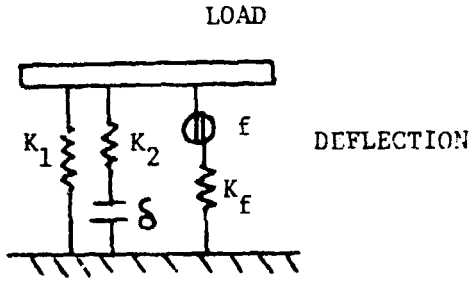

where K_1 - coil spring stiffness

K_2 - hard stop stiffness

δ - slop

f - friction

K_f - friction stiffness

This "model" yields the following load deflection picture.

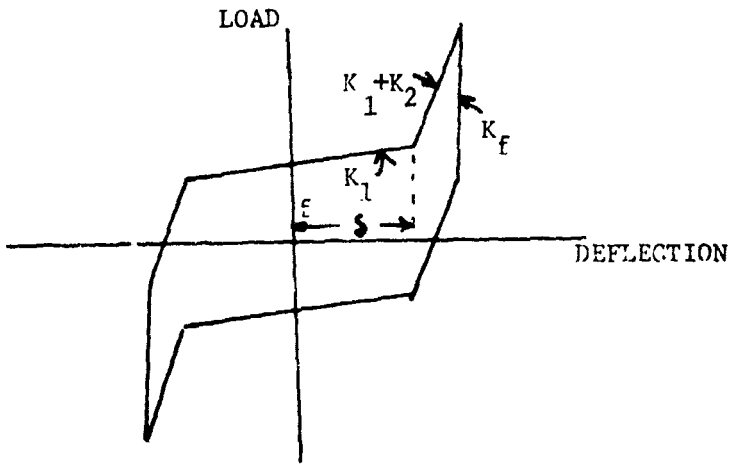

The elements of the "model" are the parameters we wish to measure. The test will provide the load deflection data in the form shown above and the "model" parameters determined directly.

The test program consisted of 3 distinct tests. These were:

1. Vertical,
2. Lateral, and
3. Warping.

In the vertical test, a vertical load was applied to the bolster and reacted at the wheels. The load was varied from 0 to 100,000 lbs and back to zero in a period of approximately 5 seconds.

In the lateral test, a lateral load was applied to the bolster and reacted at the wheels. The lateral load was varied ±10,000 lbs sinusoidally with a period of 4 seconds. Superimposed on the truck was a constant vertical load of 20,000 lbs (simulating an empty car) or 100,000 lbs (simulating a full car).

In the warping test, the truck was inverted with the bolster center plate resting on a pedestal. The constant vertical loads simulating the car weight were applied through the axles. The active loads were applied horizontally to the ends of the axles in a direction along the diagonal of the truck.

In each test the relative truck motions were measured with deflection transducers and the forces measured with load cells. The details of the test setup and procedure and data reduction may be found in Reference 1.

Comparison of Parameters

The reduced data from the tests was used to determine the parameters of the "model" for each mode of deformation. A simple computer program was written to generate analytical load deflection data and superimpose the measured data. Figures 1-13 illustrate the analytical/experimental comparison and Table I tabulates the comparison of parameters between the Barber and ASF trucks. Figure 22 illustrates the location of the instruments used for comparison. Note the numbers in the table are in a different form and are slightly different from those previously published in Reference 1. The reason for this is that a refinement was made in the correlation technique which resulted in an improved set of numbers.

Examination of Table I reveals that the major differences in the two trucks is in the friction. The construction differences indicate that this difference in friction is all due to the friction wedge. In the ASF design the friction between bolster and side frame is independent of the relative vertical displacement between bolster and side frame. In the Barber design the friction between bolster and side frame increases as the bolster moves downwards relative to the side frame.

With the specific hardware being used there results a much higher friction for the Barber truck than for the ASF truck in the fully loaded condition and similar friction for the empty condition. The merits of this situation will be discussed later in the report.

Comparison of Responses

Since the comparison of parameters did not reveal anything exciting it was decided that further analysis using the parameters was required. The basic approach was to form the equations of motion of a system containing an 80 ton Hopper car and two trucks using the following 12 degrees of freedom:

1. car lateral translation (y),
2. car yaw (θz),
3. car roll (θx),
4. car torsion mode (ξ),
5. truck translation (y_t),
6. truck yaw (θ_{z_t}),
7. truck warping (θ_w),
8. truck relative bolster lateral (y), and
9.-12. Same as 5 through 8 for other truck.

The input to this system of equations was a track misalignment model. The track misalignment was an artifically created set of random numbers with appropriate filtering to obtain the characteristic spectral shape (PSD vs wave length).

The wheel rail interactions were defined using linear creep and constant taper of the wheels.

A complete derivation of the equations of motion and wheel rail interaction may be found in Appendix A. Definition of the rail misalignment function may be found in Appendix B.

The output of the solution of the dynamic equations of motion used as a basis of comparison were the loads generated between wheel and rail. Figures 14 through 19 illustrate the time histories of loads for typical runs. The comparison was made simply by examining the peak values of the time histories. As in the case of the parameter comparison there is no dramatic difference.

Limitations of Model

The model used for the comparison of the two trucks is based on a test program where the characteristics are measured independently. In a nonlinear system this type of measurement does not necessarily provide a unique result. The Operational test which we are to run as a part of our Track-Train Dynamics contract will provide the answer to this question.

Another limitation of the model is the neglect of the coupling between vertical and roll motions of the bolster due to the friction.

Consider the equilibrium of the wedge for the bolster moving down with respect to the side frame and vice versa.

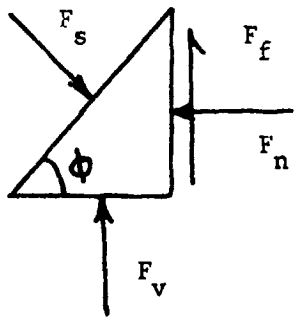

Downward motion

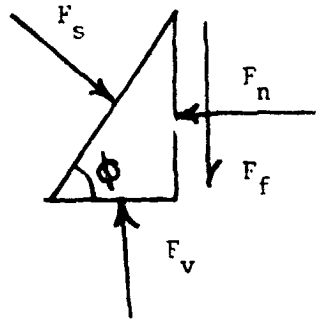

Upward motion

$$F_f = \mu F_n = \frac{\mu F_v}{\tan\phi - \mu}$$

$$F_f = \mu F_n = \frac{\mu F_v}{\tan\phi + \mu}$$

When the bolster rolls with respect to the frames, there results a net vertical force due to the difference in force between the two sides.

All of this is pointed out so that any future work either analytical or experimental may possibly remove some of these limitations.

Conclusions

The comparisons which have been made between the Barber S-2 and the ASF ride control trucks indicates only small differences in parameters and response to rail irregularities. This may also be verified physically since the construction of the trucks is very similar. The major difference in the two trucks exists in the area of the friction wedge. The difference is small for the unloaded trucks and large for the fully loaded trucks.

The response differences may be accentuated if vertical degrees of freedom were included in the mathematical models with the coupling caused by the friction wedge behavior. Future work with nonlinear models should consider this phenomenon.

The load/deflection data generated in this program is limited by the manner in which it was obtained, ie., by testing the modes of deformation independently. In the configurations tested, the friction parameter (the only real source of energy dissipation in the hardware)

will probably be affected by the superposition of modes of deformation. Our test setup would not handle this kind of test, hence, the limitations or uncertainties of the results.

Finally, it should be pointed out that friction is a simple but strange phenomenon which, in some cases, will not dissipate as much energy as thought. For instance, in the case of the friction wedge, suppose there is vertical motion of the bolster relative to the side frame caused by track vertical irregularities, then very little lateral force is required to cause motion. As a matter of fact the lateral friction appears to be viscous, in this case, with a coefficient equal to the friction force divided by the magnitude of vertical velocity. Other combinations of motion such as roll and vertical can cause similarly strange results.

REFERENCES

1. Martin Marietta Report, TR-006 3 Test Report, Track Train Dynamics Analysis and Test Program - Barber S-2 Static Test - February 1976

2. Clemson/ASU Report Parametric Study of Freight Car Stability - Preliminary Results, Contract DOT-05-40018, "Freight Car Dynamics"

3. Law, E. H., Nonlinear Wheelset Dynamic Response to Random Lateral Rail Irregularities, ASME Paper No. 73-WA/RT-3, November 1973

APPENDIX A - MATHEMATICAL MODEL

The mathematical model of the rail-truck-car system used for this study is comprised of the following ingredients.

1. equations of motion of car,
2. equations of motion of trucks,
3. compatibility relations between car and trucks, and
4. linear creep equations and assumptions for wheel/rail force determination.

Equations of Motion of Car

For the purposes of a lateral analysis, the following 4 degrees of freedom (modes of motion) are used to describe the car absolute motions:

1. lateral translation (Y)
2. yaw (θ_z)
3. roll (θ_x)
4. first torsion mode (free-free) (ξ)

The equations of motion become (in matrix form)

$$\begin{bmatrix} M & & & \\ & I_Y & & \\ & & I_r & \\ & & & M_T \end{bmatrix} \begin{Bmatrix} \ddot{Y} \\ \theta_z \\ \theta_x \\ \xi \end{Bmatrix} + \begin{bmatrix} 0 & & & \\ & 0 & & \\ & & 0 & \\ & & & 2\zeta M_T \omega \end{bmatrix} \begin{Bmatrix} \dot{Y} \\ \theta_z \\ \theta_x \\ \xi \end{Bmatrix} +$$

$$\begin{bmatrix} 0 & & & \\ & 0 & & \\ & & 0 & \\ & & & M_T\omega^2 \end{bmatrix} \begin{Bmatrix} Y \\ \theta_z \\ \theta_x \\ \xi \end{Bmatrix} = \begin{bmatrix} \delta Y_Y & \delta\theta_{zY} & & \\ \delta Y_{\theta_z} & \cdots & & \\ \cdots & & & \\ & & \text{etc.} & \end{bmatrix} \begin{Bmatrix} F_1 \\ M_{Y1} \\ M_{r1} \\ F_2 \\ M_{Y2} \\ M_{R2} \end{Bmatrix}$$

Where,

M - mass of car

I_y - yaw inertia about c.g.

I_r - roll inertia about c.g.

M_t - generalized mass of torsion mode

ζ - % of critical damping of torsion mode

ω - natural frequency of torsion mode

F - lateral force between car and truck

M_y - yaw moment between car and truck

M_r - roll moment between car and truck

δY_i - mode shape (lateral displacement) in the ith mode

$\delta \theta_{z_i}$ - mode shape (yaw) in the ith mode

$\delta \theta_{x_i}$ - mode shape (roll) in the ith mode

Equations of Motion of Trucks

The truck model is also described by 4 degrees of freedom. These are:

1. lateral translation y_t,
2. yaw θ_{yt},
3. warping θ_w ,
4. bolster relative lateral $\bar{y}$

The equations of motion for the truck are derived in a slightly different form than for the car for ease in handling the nonlinear characteristics of the warping and relative lateral modes. This is done by defining the motion of the truck pieces as the motion of some arbitrary reference point plus the motion due to warping and relative lateral. This is similar to the approach taken in linear modal coupling and results in a set of equations coupled in the mass matrix and uncoupled in the stiffness matrix. This form greatly simplifies the handling of the nonlinear load deflection relationships.

Taking the standard Lagrange equation approach the acceleration terms (mass matrix) are defined by

$$\frac{d}{dt}\left(\frac{\partial T}{\partial \dot{q}_i}\right)$$

Where,

T - kinetic energy

$\frac{\partial}{\partial \dot{q}_i}$ - partial derivative with respect to generalized velocity

$\frac{d}{dt}$ - derivative with respect to time

The total kinetic energy is defined as the sum of the kinetic energy of the truck pieces

$$T = T_{bolster} + T_{\substack{left\ side \\ frame}} + T_{\substack{right\ side \\ frame}} + T_{\substack{front \\ axle}} + T_{\substack{rear \\ axle}}$$

We select the arbitrary reference point as the center of gravity of the rear axle. Hence, the velocities of a point on the various pieces may be written

$$\dot{x}_{ra_i} = -y_i \dot{\theta}_z$$
$$\dot{y}_{ra_i} = \dot{y} + x_i \dot{\theta}_z$$

$$\dot{x}_{rsf_i} = -y_{rsf_i} \dot{\theta}_z$$
$$\dot{y}_{rsf_i} = \dot{y} + x_i(\dot{\theta}_z + \dot{\theta}_w)$$

$$\dot{x}_{b_i} = -y_i \dot{\theta}_z$$
$$\dot{y}_{b_i} = \dot{y} + x_b(\dot{\theta}_z + \dot{\theta}_w) + \dot{\bar{y}}$$

$$\dot{x}_{fa_i} = -y_i \dot{\theta}_z$$
$$\dot{y}_{fa_i} = \dot{y} + x_{fa}(\dot{\theta}_z + \dot{\theta}_w)$$

where

$\dot{x}_{ra_i}$ - x direction velocity of i<u>th</u> point on rear axle

y_i - y location of i<u>th</u> point

etc.

subscript

ra - rear axle

rsf - right side frame

b - bolster

fa - front axle

lsf - left side frame

The kinetic energy for the Kth piece is given by

$$T_K = \frac{1}{2} \sum_{i=1}^{n} m_{iK} \dot{q}_{iK}^2$$

for the rear axle

$$T_{ra} = \frac{1}{2} \sum_{i=1}^{n} m_i \left(-y_i \dot{\theta}_z\right)^2 + \frac{1}{2} \sum_{i=1}^{n} m_i \left(\dot{y} + x_i \dot{\theta}_z\right)^2$$

$$\frac{\partial T_{ra}}{\partial \dot{\theta}_z} = \sum_{i=1}^{n} m_i y_i^2 \dot{\theta}_z + \sum_{i=1}^{n} m_i (\dot{y} + x_i \dot{\theta}_z) x_i$$

since $\sum m_i x_i = 0$ there results

$$\frac{\partial T_{ra}}{\partial \dot{\theta}_z} = \sum m_i (x_i^2 + y_i^2) \dot{\theta}_z = I_{zra} \dot{\theta}_z$$

I_z - yaw moment of inertia of rear axle

$$\frac{d}{dt} \frac{\partial T_{ra}}{\partial \dot{\theta}_z} = I_{zra} \ddot{\theta}_z$$

This procedure is carried out for all pieces and all coordinates (y, θ_z, θ_ω, $\bar{y}$) and results in the following mass matrix

$$\begin{bmatrix} M_T & M_T \bar{X} & M_T \bar{X} & M_b \\ & I_T & I_P & M_b \bar{X}_b \\ \text{SYM.} & & I_P & M_b \bar{X}_b \\ & & & M_b \end{bmatrix}$$

where

M_T - total truck mass

$\bar{X}$ - center of gravity of truck with respect to reference point

M_b - bolster mass

I_T - total truck yaw inertia

I_P - partial yaw inertia (does not contain c.g. inertias of bolster and front axle)

$\bar{X}_b$ - bolster c.g. with respect to reference point

The complete equations of motion for the truck becomes (in general)

$$M\ddot{q} + LD(X,\dot{X}) = -F_{CT} + F_{wr}$$

where

M - mass matrix

$\ddot{q}$ - generalized coordinate accelerations

$LD(X,\dot{X})$ - nonlinear load deflection characteristics

F_{CT} - forces between car and truck

F_{wr} - forces between wheel and rail

The car/truck lateral forces are determined by a nonlinear load deflection relation depicted below

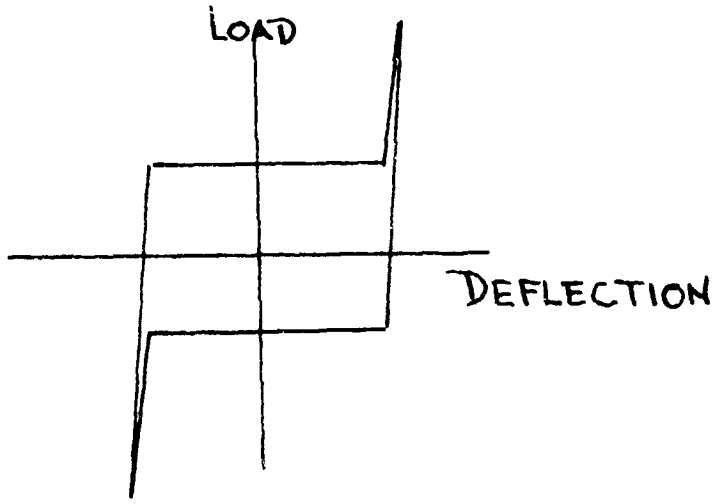

This physically represents the center plate friction and the lip contact after ±1/8 inch of motion. In yaw the phenomenon is pure friction.

The wheel rail forces are defined assuming linear creep with constant tapered wheels.

The generalized force due to rail motion

$$G = \phi^T F$$

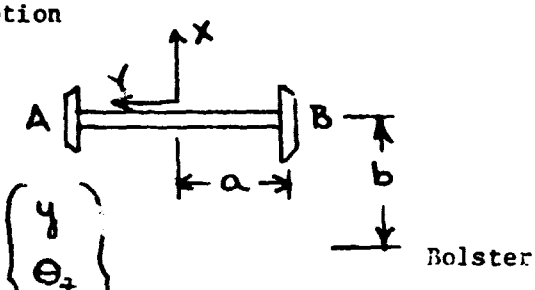

$$\phi = \begin{Bmatrix} X_A \\ Y_A \\ X_B \\ Y_B \end{Bmatrix} = \begin{bmatrix} 0 & -a & 0 & 0 \\ 1. & b & b & 0 \\ 0 & a & 0 & 0 \\ 1. & b & b & 0 \end{bmatrix} \begin{Bmatrix} y \\ \theta_z \\ \theta_w \\ \bar{y} \end{Bmatrix}$$

$$\phi^T F = -f_c \begin{bmatrix} 0 & -2. \\ \frac{-2a\alpha}{r_o} & -2b \\ 0 & -2b \\ 0 & 0 \end{bmatrix} \begin{Bmatrix} y_{rail} \\ \theta_{rail} \end{Bmatrix}$$

where ,

f_c - creep coefficient

r_o - wheel radius

α - wheel taper (.05)

rear axle looks same b=0.

Total

$$\phi^T F = -f_c \begin{bmatrix} 0 & -4 \\ \frac{-4a\alpha}{r_o} & -2b \\ 0 & -2b \\ 0 & 0 \end{bmatrix} \begin{Bmatrix} y_{rail} \\ \theta_{rail} \end{Bmatrix}$$

<u>Forces</u> - The wheel rail forces are given

$$\left\{ f \right\} = -\frac{f_c}{V} \left\{ \bar{V} \right\} \qquad \begin{array}{l} \bar{V} \text{ - relative velocity} \\ V \text{ - forward velocity} \end{array}$$

The relative velocity for an axle is the modal motion plus the track

<u>Rear axle</u>

$$\begin{Bmatrix} f_{AX} \\ f_{AY} \\ f_{BX} \\ f_{BY} \end{Bmatrix} = -\frac{f_c}{V} \begin{bmatrix} -\frac{V\alpha}{r_o} & 0 & 0 & 0 \\ 0 & -V & 0 & 0 \\ \frac{V\alpha}{r_o} & 0 & 0 & 0 \\ 0 & -V & 0 & 0 \end{bmatrix} \begin{Bmatrix} y \\ \theta_y \\ \theta_w \\ \bar{y} \end{Bmatrix}$$

$$-\frac{f_c}{V} \begin{bmatrix} 0 & -a & 0 & 0 \\ 1. & 0 & 0 & 0 \\ 0 & a & 0 & 0 \\ 1. & 0 & 0 & 0 \end{bmatrix} \begin{Bmatrix} \dot{y} \\ \dot{\theta}_z \\ \dot{\theta}_w \\ \dot{\bar{y}} \end{Bmatrix}$$

$$-f_c \begin{bmatrix} 0 & -2 \\ -\frac{2\alpha}{r_o} & 0 \\ 0 & 0 \\ 0 & 0 \end{bmatrix} \begin{Bmatrix} y_{rail} \\ \theta_{rail} \end{Bmatrix}$$

<u>for the front axle</u>

$$\begin{Bmatrix} f_{AX} \\ f_{AY} \\ f_{BX} \\ f_{BY} \end{Bmatrix} = -f_c \begin{bmatrix} -\frac{\alpha}{r_o} & -\frac{b\alpha}{r_o} & -\frac{b\alpha}{r_o} & 0 \\ 0 & -1. & 0 & 0 \\ \frac{\alpha}{r_o} & \frac{b\alpha}{r_o} & \frac{b\alpha}{r_o} & 0 \\ 0 & -1. & 0 & 0 \end{bmatrix} \begin{Bmatrix} Y \\ \theta_z \\ \theta_w \\ \bar{Y} \end{Bmatrix}$$

$$-\frac{f_c}{V}\begin{bmatrix} 0. & -a & 0 & 0 \\ 1. & b & b & 0 \\ 0 & a & 0 & 0 \\ 1. & b & b & 0 \end{bmatrix}\begin{Bmatrix} \dot{Y} \\ \theta_z \\ \theta_w \\ \bar{Y} \end{Bmatrix} - f_c\begin{bmatrix} \alpha/r_0 & 0 \\ 0 & -1. \\ -\frac{\alpha}{r_0} & 0 \\ 0 & -1. \end{bmatrix}\begin{Bmatrix} y_{rail} \\ \theta_{rail} \end{Bmatrix}$$

Finally, the rail loads matrices

$$T^T f = \begin{Bmatrix} f_Y \\ M_Y \end{Bmatrix}$$

total force on axle

total moment about axle center

$$T = \begin{bmatrix} 0 & -a \\ 1. & 0 \\ 0 & a \\ 1. & 0 \end{bmatrix}$$

$$T^T f = \begin{bmatrix} 0 & 1. & 0 & 1. \\ -a & 0 & a & 0 \end{bmatrix}\begin{Bmatrix} f \end{Bmatrix}$$

multiplying by matrices at bottom of page 15

$$\{X_L\} = f_c\begin{bmatrix} 0 & 2. & 0 & 0 \\ -\frac{2a\alpha}{r_0} & -\frac{2ba\alpha}{r_0} & -\frac{2ba\alpha}{r_0} & 0 \end{bmatrix}\begin{Bmatrix} Y \\ \theta_z \\ \theta_w \\ \bar{Y} \end{Bmatrix}$$

$$\{XD_L\} = \frac{f_c}{V}\begin{bmatrix} -2 & -2b & -2b & 0 \\ 0 & -2a^2 & 0 & 0 \end{bmatrix}\begin{Bmatrix} \dot{Y} \\ \theta_z \\ \theta_w \\ \bar{Y} \end{Bmatrix}$$

$$\{X_R\} = f_c\begin{bmatrix} 0 & 2 \\ \frac{2a\alpha}{r_0} & 0 \end{bmatrix}\begin{Bmatrix} Y_{rail} \\ \theta_{rail} \end{Bmatrix}$$

The resulting equations of motion were integrated numerically on a CDC 6500 digital computer.

APPENDIX B - RANDOM RAIL MODEL

Reference 3 gives typical rail lateral alignment spectral densities as a function of spatial frequency or 1/wave-length. A reasonable approximation to the spectral density curve is a $1/f^2$ relationship for wavelengths between 10 and 100 feet. Below that frequency it is assumed that the spectrum is constant.

The data for use in the analysis, which fits the spectral shape was generated by creating a set of normally distributed random numbers and low pass filtering. Figure 20 illustrates the resulting Power Spectral Density vs spatial frequency. The RMS value of displacement for this PSD is .07 inches. Figure 21 illustrates the actual displacement spatial distribution.

Mode		K_1 Barber	K_1 ASF	K_2 Barber	K_2 ASF	K_f Barber	K_f ASF	Friction (f) Barber	Friction (f) ASF	Slop (δ) Barber	Slop (δ) ASF
Vertical		45000 lb/in	42857 lb/in	—		$1.\times10^6$ lb/in	$1.\times10^6$ lb/in	Varies 5000 to 15000 lb over range of vertical load	7000 lb	Spring travel limit	Spring travel limit
Roll		6.84×10^7 in lb/rad	6.51×10^7 in lb/rad	—		$1.\times10^9$ in lb/rad	$1.\times10^9$ in lb/rad				
Lateral											
Preload	20000 lb	12000 lb/in	10700 lb/in			3.9×10^5 lb/in	3.3×10^5 lb/in	5000 lb	7300 lb	Gib Clearance Limit	Gib Clearance Limit
	50000 lb	16000	15700			3.5×10^5	3.5×10^5	12000	6800		
	100000 lb	28000	27700			4.2×10^5	4.2×10^5	15000	6000		
Warping											
Preload	20000 lb	1.88×10^7 in lb/rad	4.43×10^7	$5.\times10^7$ in lb/rad	5.15×10^7	1.2×10^8 in lb/rad	$3.\times10^8$	$.78\times10^5$ in lb	$.6\times10^5$	.125	Degrees .125
	50000 lb	6.02×10^7	3.83×10^7	$15.\times10^7$	$6.\times10^7$	2.4×10^8	2.85×10^8	1.58×10^5	1.1×10^5	.125	.125
	100000 lb	7.0×10^7	3.43×10^7	$18.\times10^7$	$7.\times10^7$	2.59×10^8	2.574×10^8	2.7×10^5	1.4×10^5	.125	.125

TABLE I. JOINT PARAMETERS

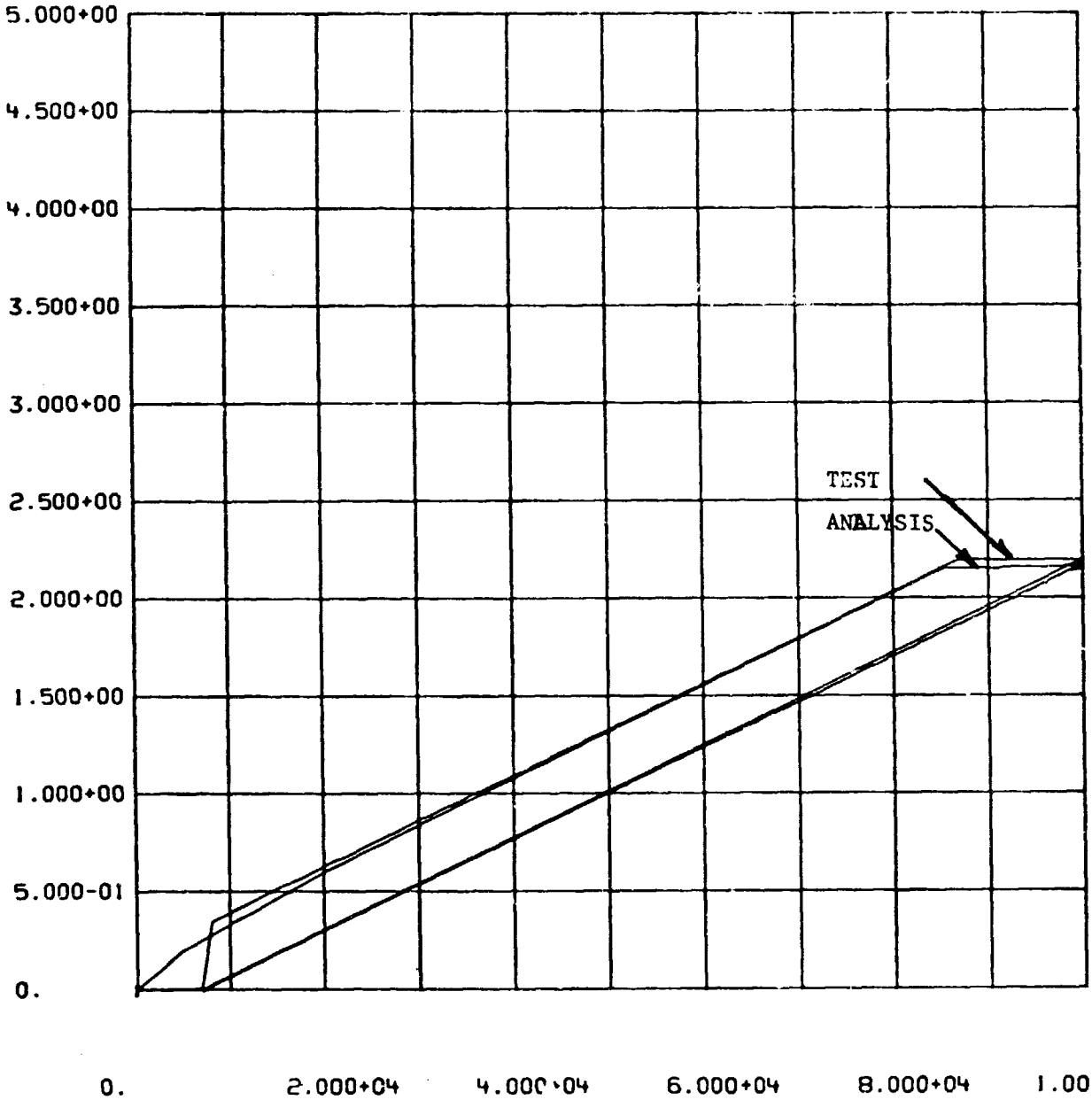

D12 VS FORCE

1 ASFVER 20AP76 ASF VERTICAL CHECK

FIGURE 1. ANALYSIS VERSUS TEST MEASUREMENT D12 ASF VERTICAL TEST

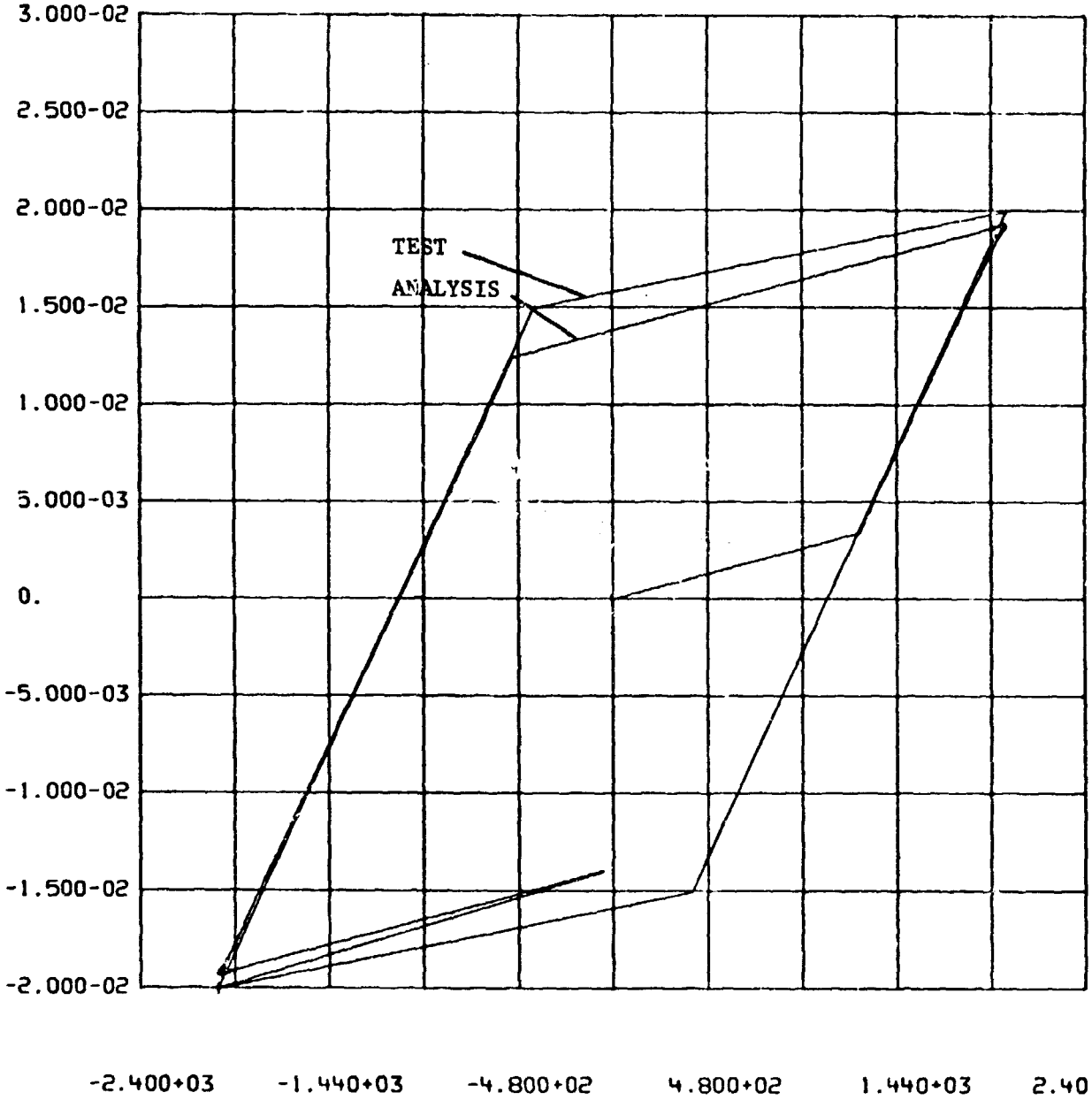

D2 VS FORCE

1 ASFWRP 20AP76 ASF WARP CHECK 20K PRELOAD

FIGURE 2. ANALYSIS VERSUS TEST MEASUREMENT D2 ASF WARP TEST 20K PRELOAD

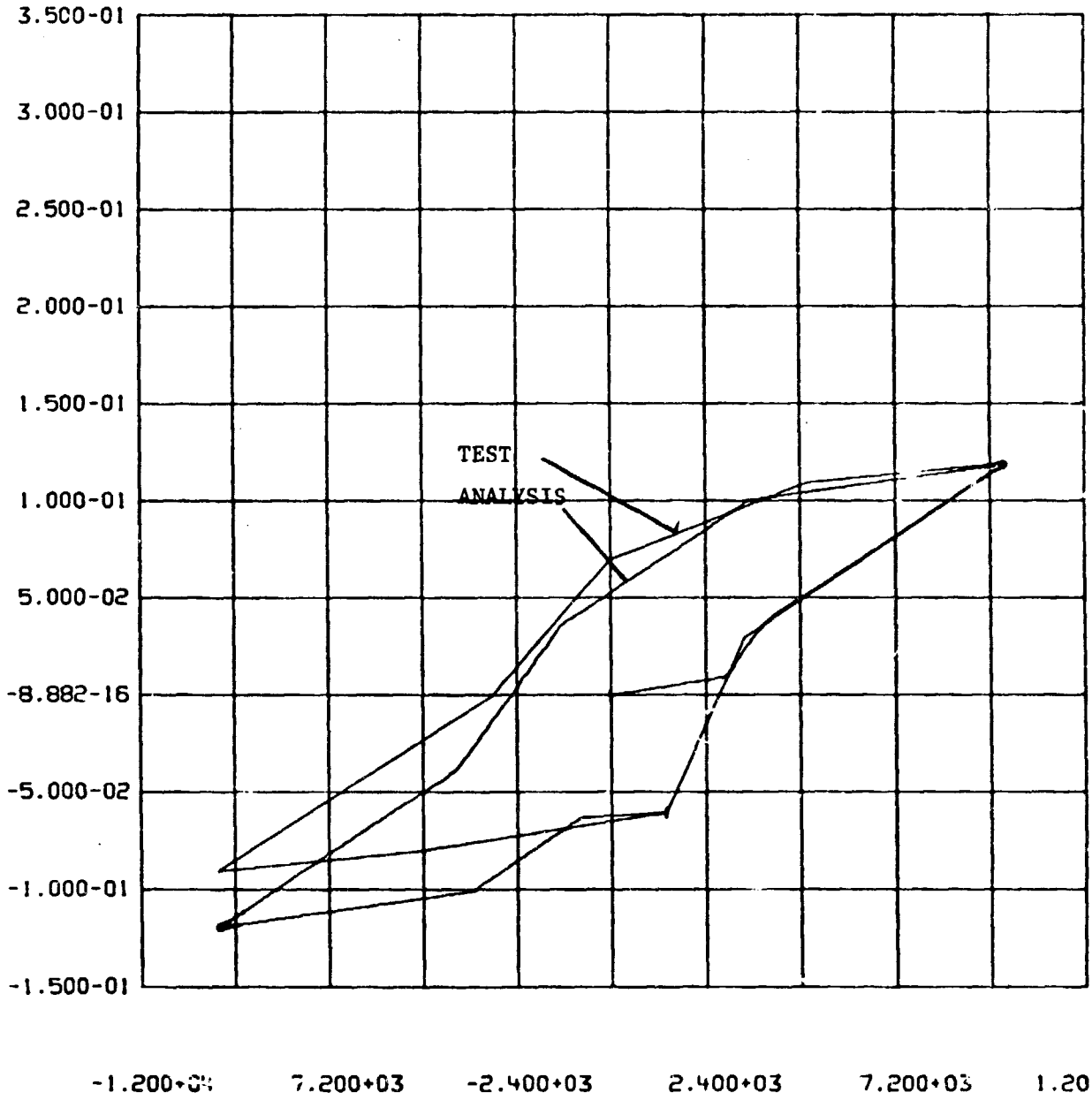

D2 VS FORCE

1 ASFWRP 20AP76 ASF WARP CHECK 100K PRELOAD

FIGURE 3. ANALYSIS VERSUS TEST MEASUREMENT D2 ASF WARP TEST 100K PRELOAD

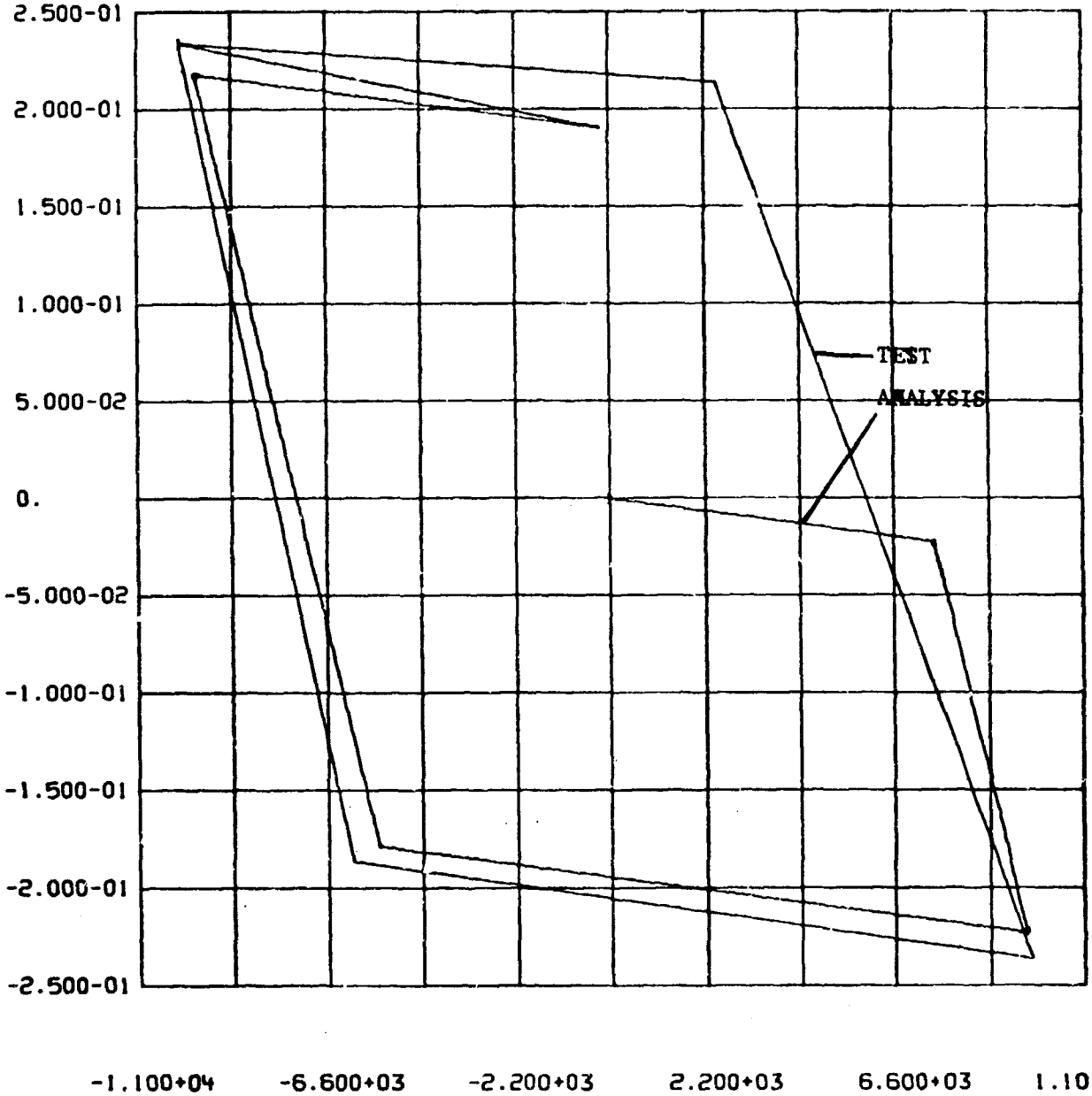

D18 VS FORCE

1 ASFLAT 20AP76 ASF LATERAL CHE CK 20K PRELOAD

FIGURE 4. ANALYSIS VERSUS TEST MEASUREMENT D18 ASF LATERAL TEST 20K PRELOAD

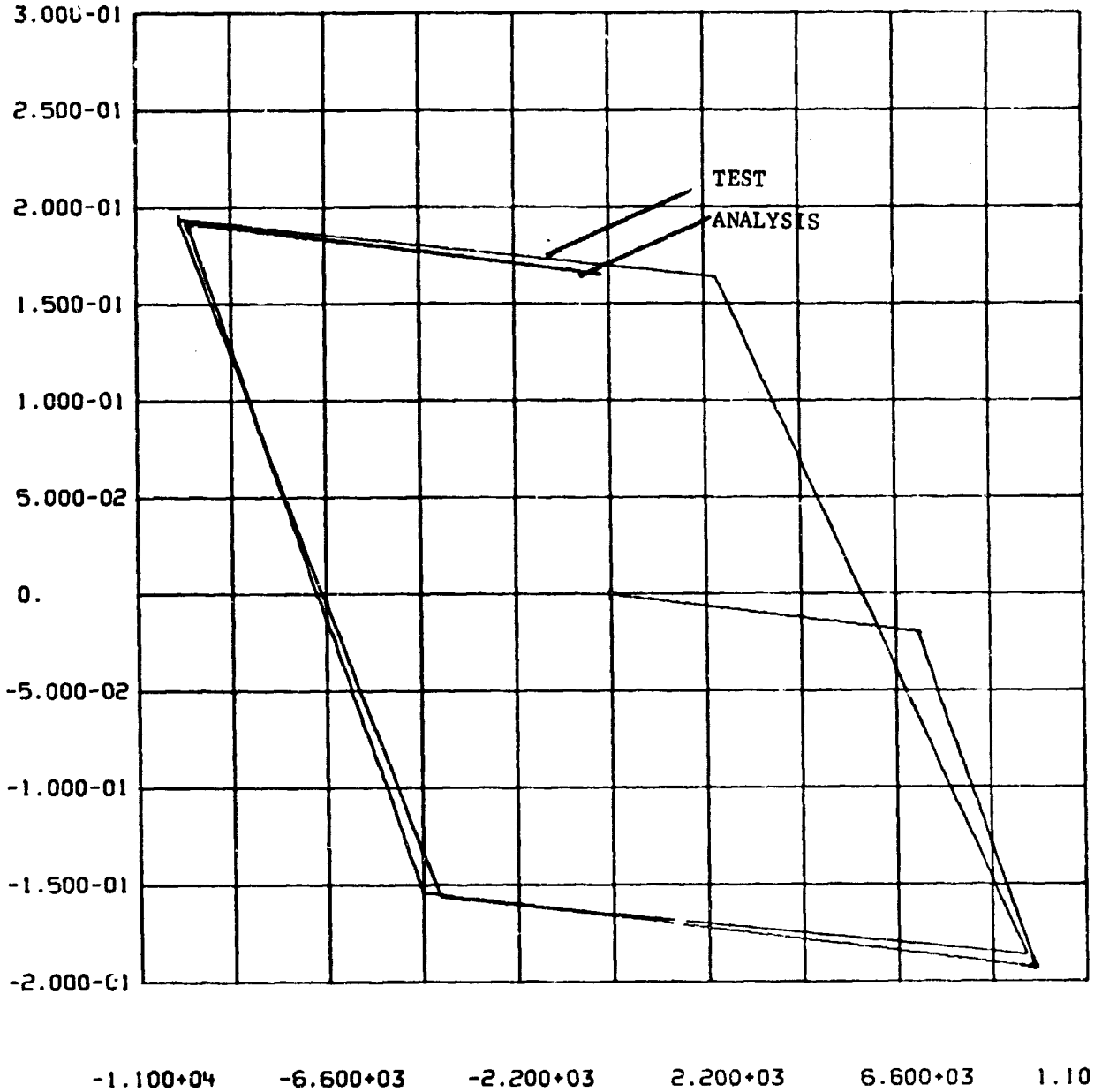

D18 VS FORCE

1 ASFLAT 20AP76 ASF LATERAL CHECK 50K PRELOAD

FIGURE 5. ANALYSIS VERSUS TEST MEASUREMENT D18 ASF LATERAL TEST 50K PRELOAD

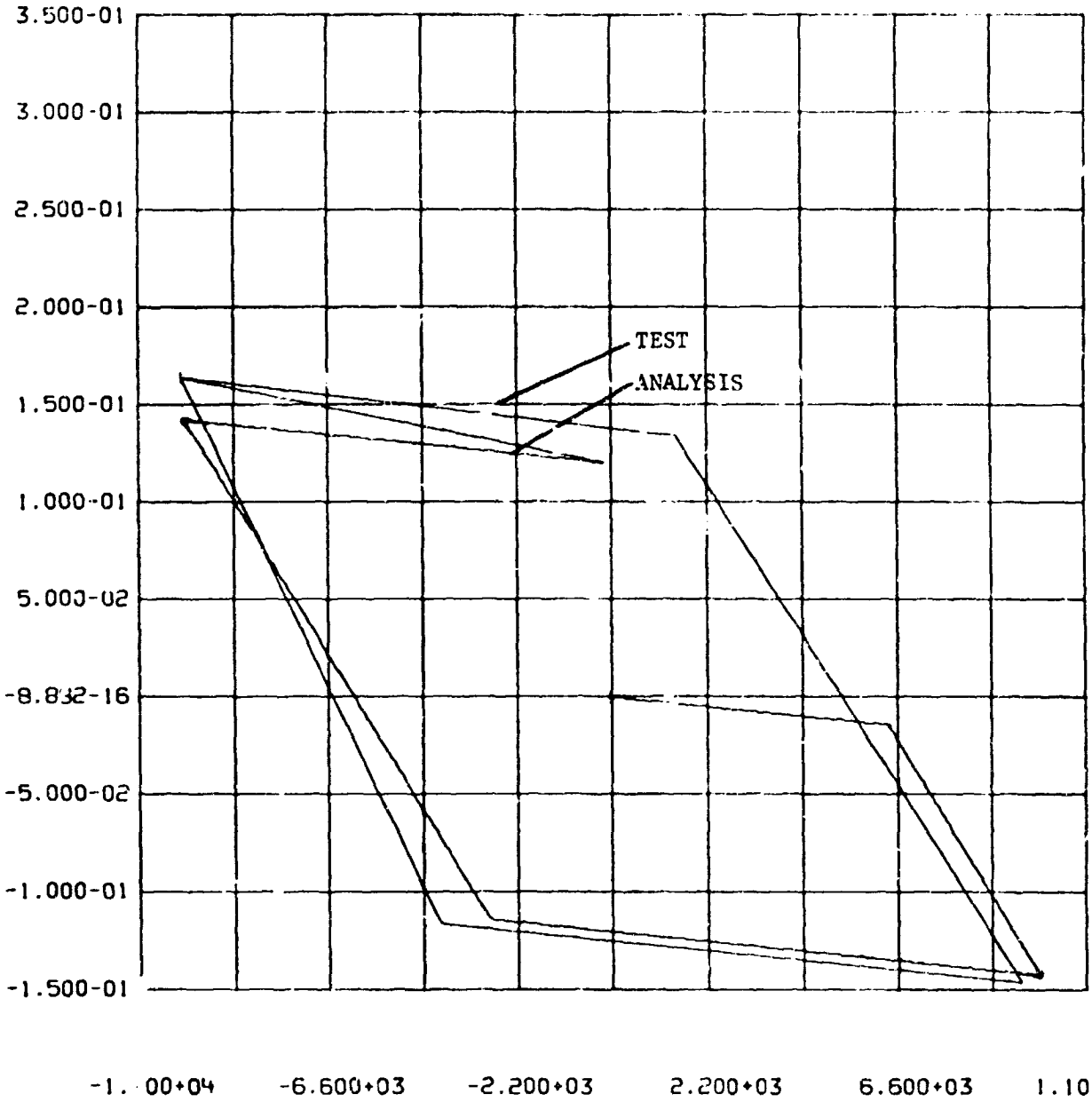

D18 VS FORCE

1 ASFLAT 20AP76 ASF LATERAL CHECK 100K PRELOAD

FIGURE 6. ANALYSIS VERSUS TEST MEASUREMENT D18 ASF LATERAL TEST 100K PRELOAD

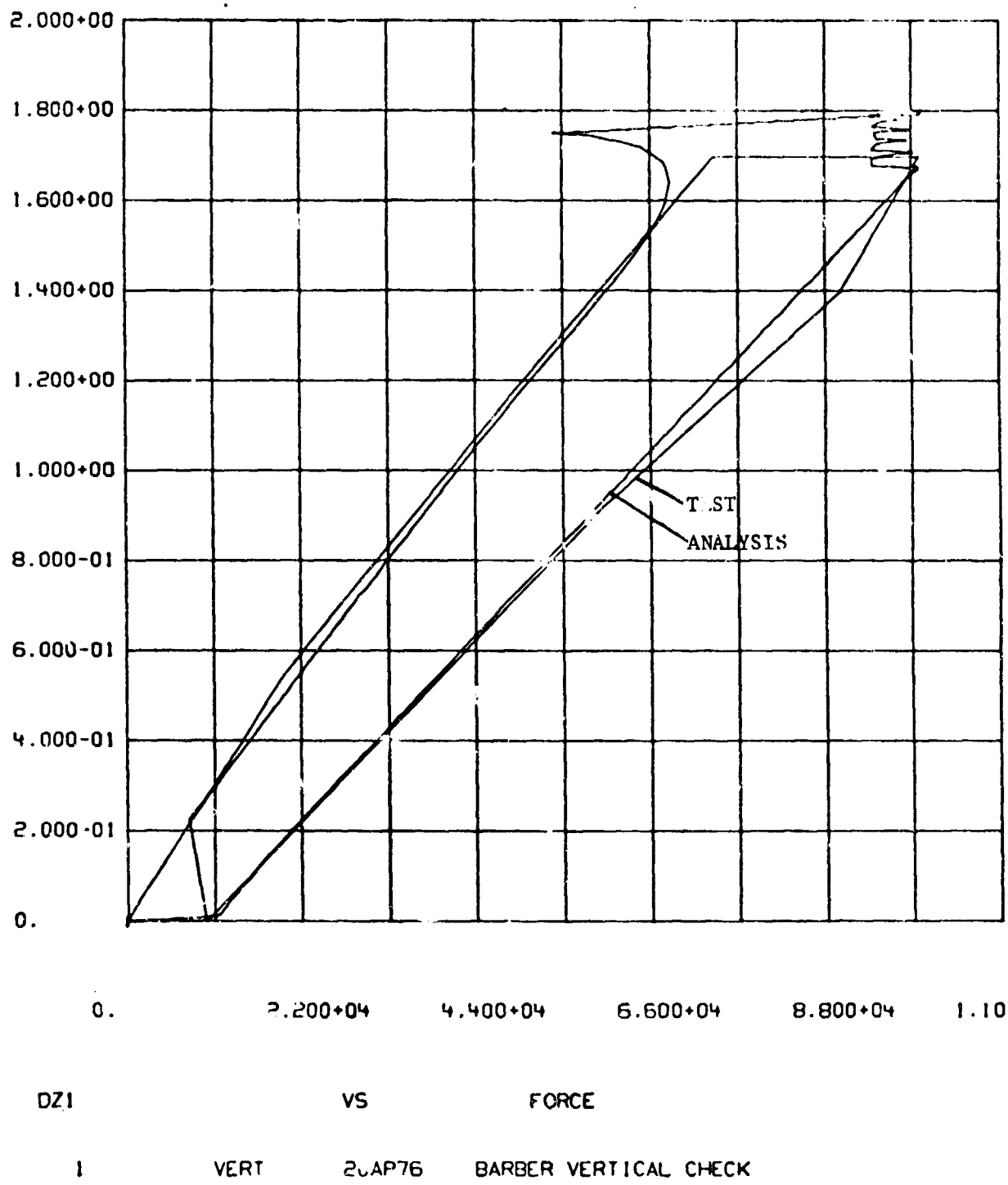

FIGURE 7. ANALYSIS VERSUS TEST MEASUREMENT DZ1. BARBER VERTICAL TEST

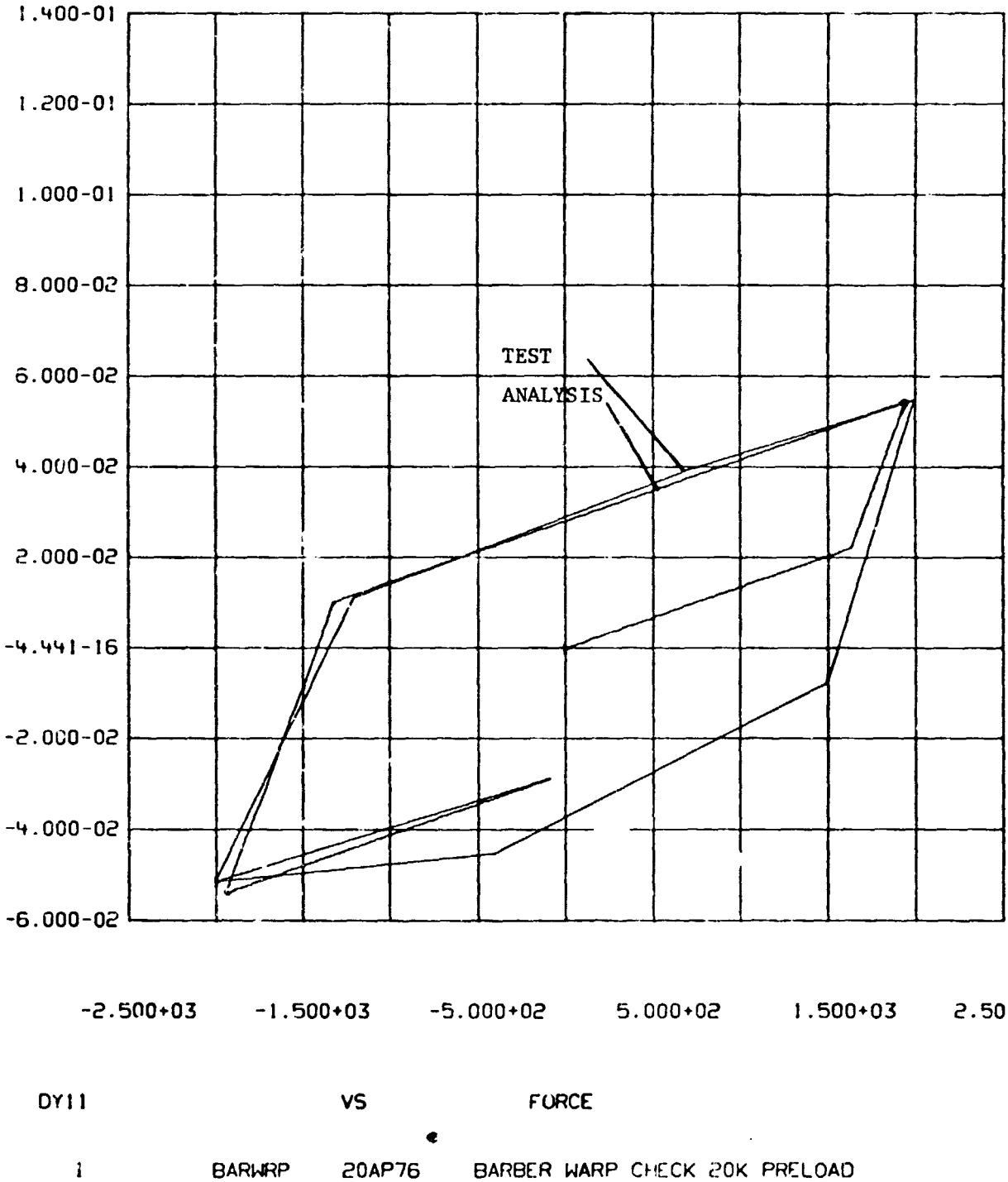

FIGURE 8. ANALYSIS VERSUS TEST MEASUREMENT DY11 BARBER WARP TEST 20K PRELOAD

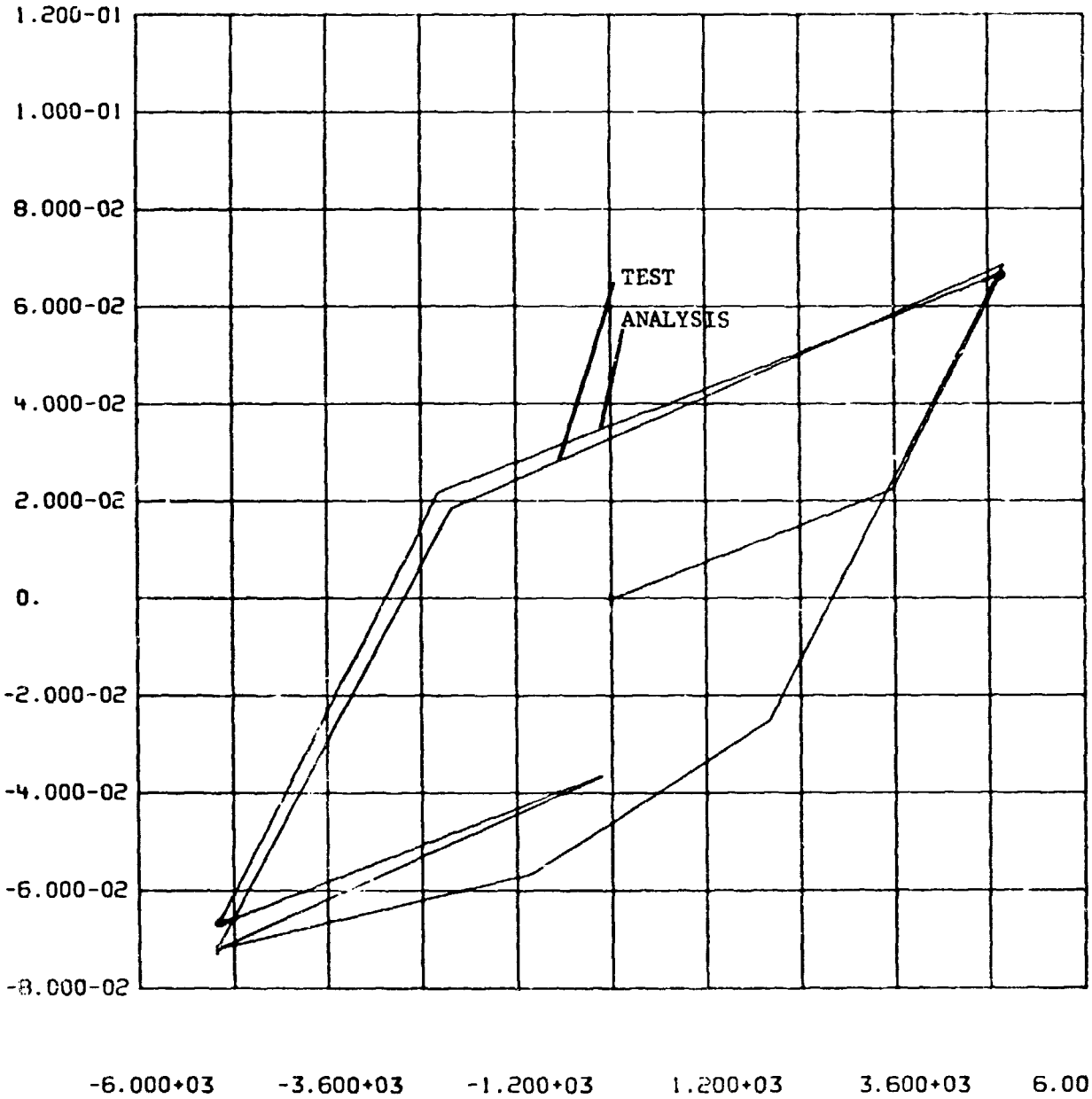

DY11 VS FORCE

1 BARWRP 20AP76 BARBER WARP CHECK 50K PRELOAD

FIGURE 9. ANALYSIS VERSUS TEST MEASUREMENT DY11 BARBER WARP TEST 50K PRELOAD

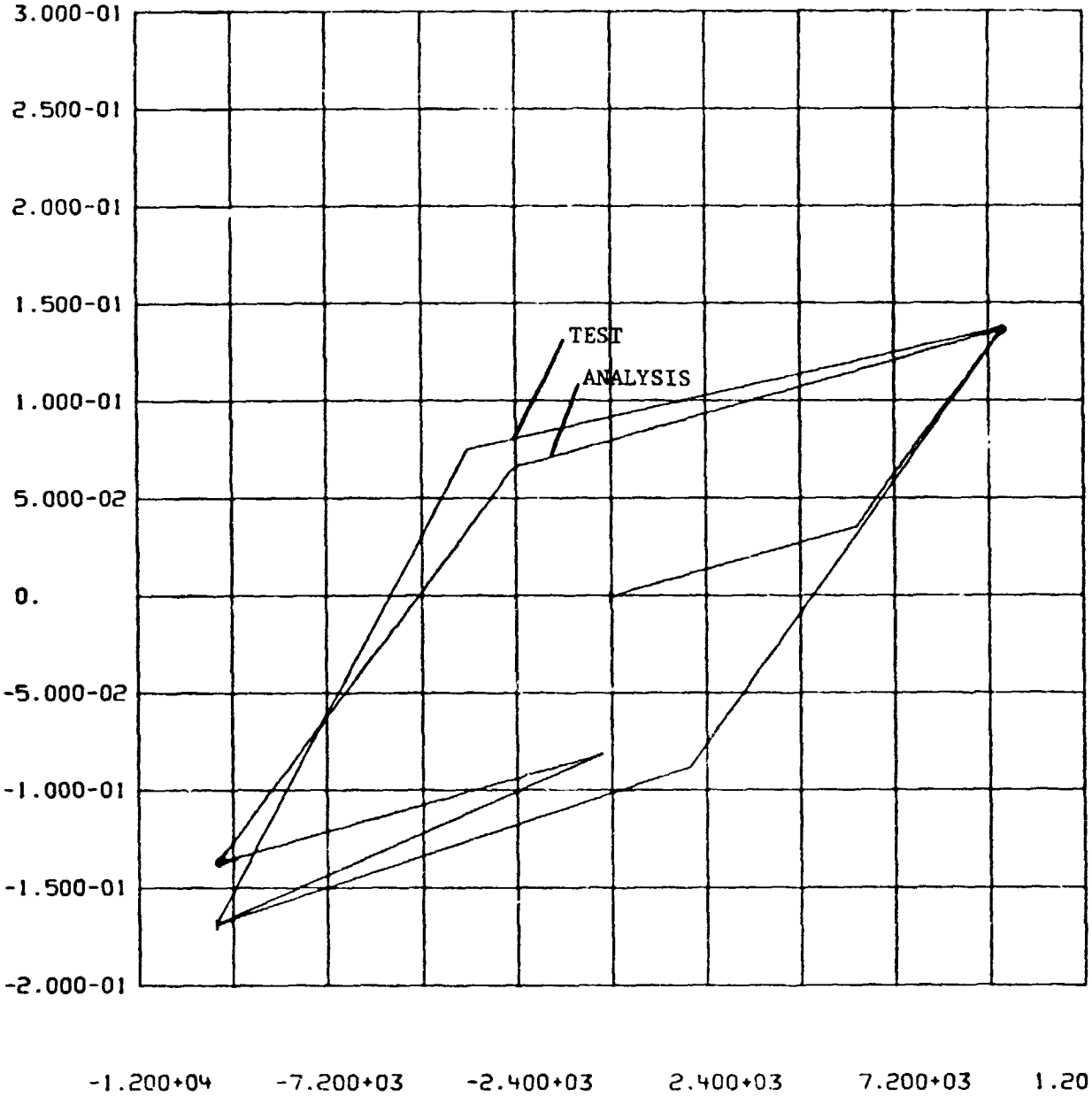

DY11 VS FORCE

1 BARWRP 20AP76 BARBER WARP CHECK 100K PRELOAD

FIGURE 10. ANALYSIS VERSUS TEST MEASUREMENT DY11 BARBER WARP TEST 100K PRELOAD

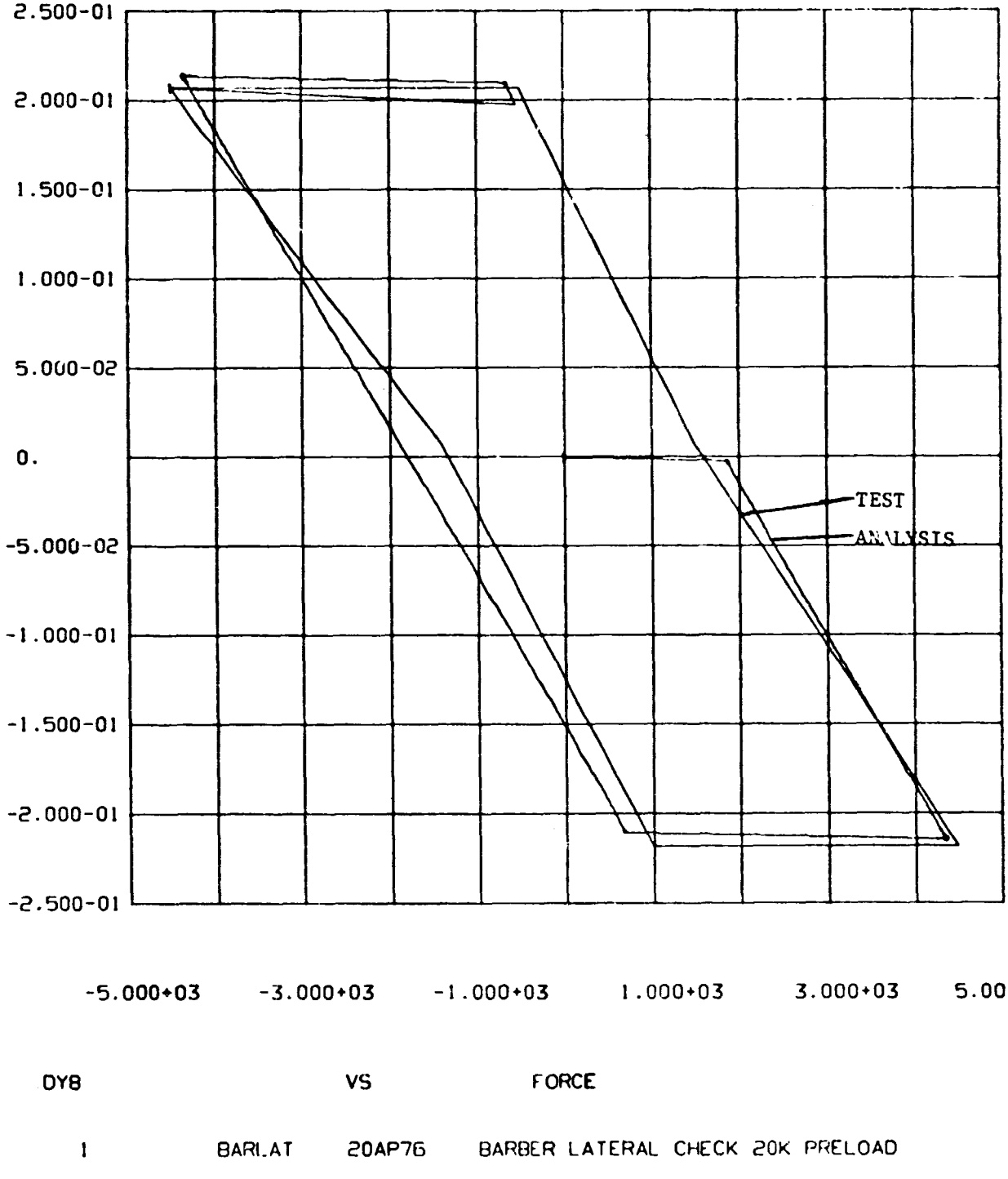

FIGURE 11. ANALYSIS VERSUS TEST MEASUREMENT DY8 BARBER LATERAL TEST 20K PRELOAD

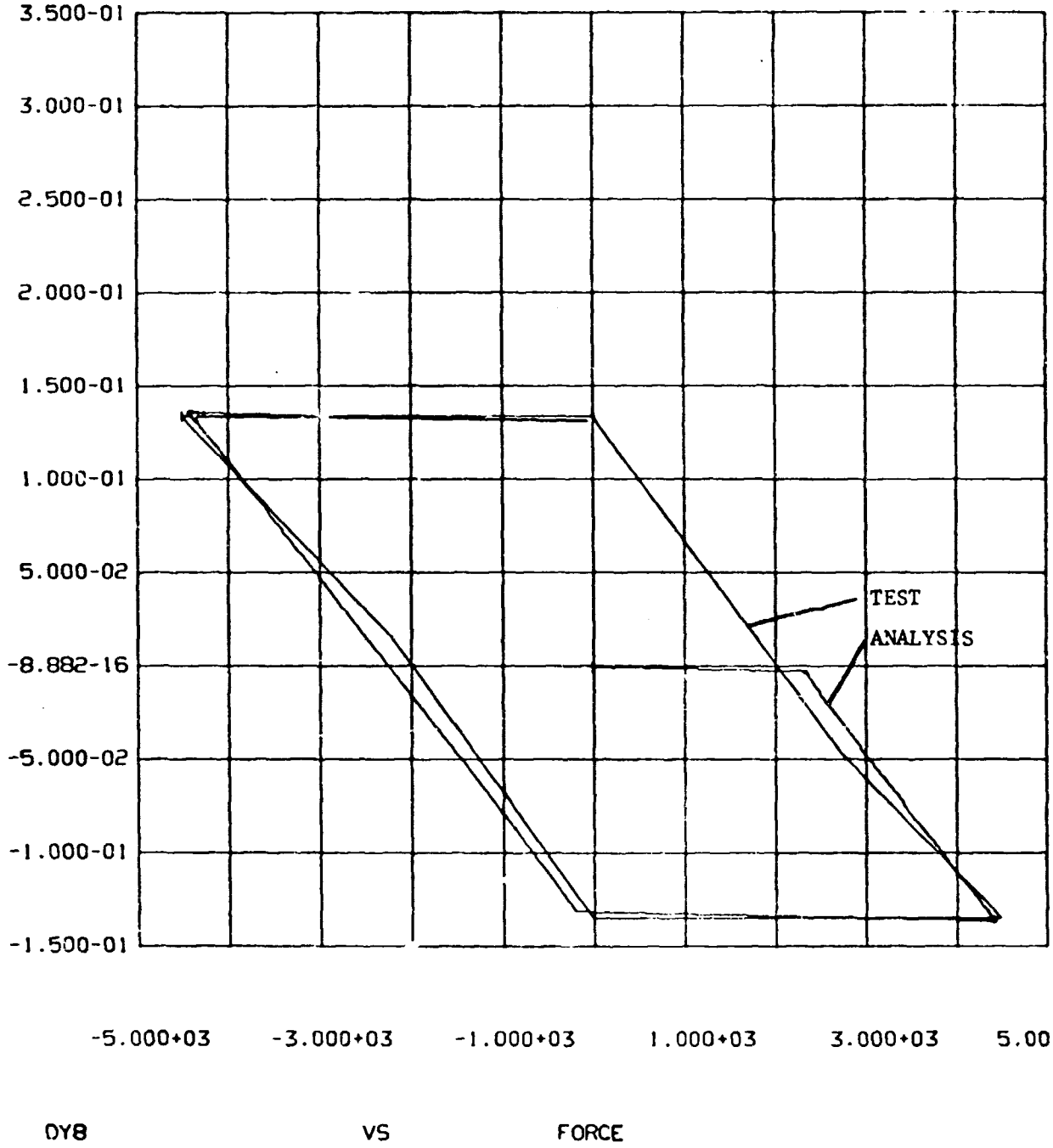

FIGURE 12. ANALYSIS VERSUS TEST MEASUREMENT DY8 BARBER LATERAL TEST 50K PRELOAD

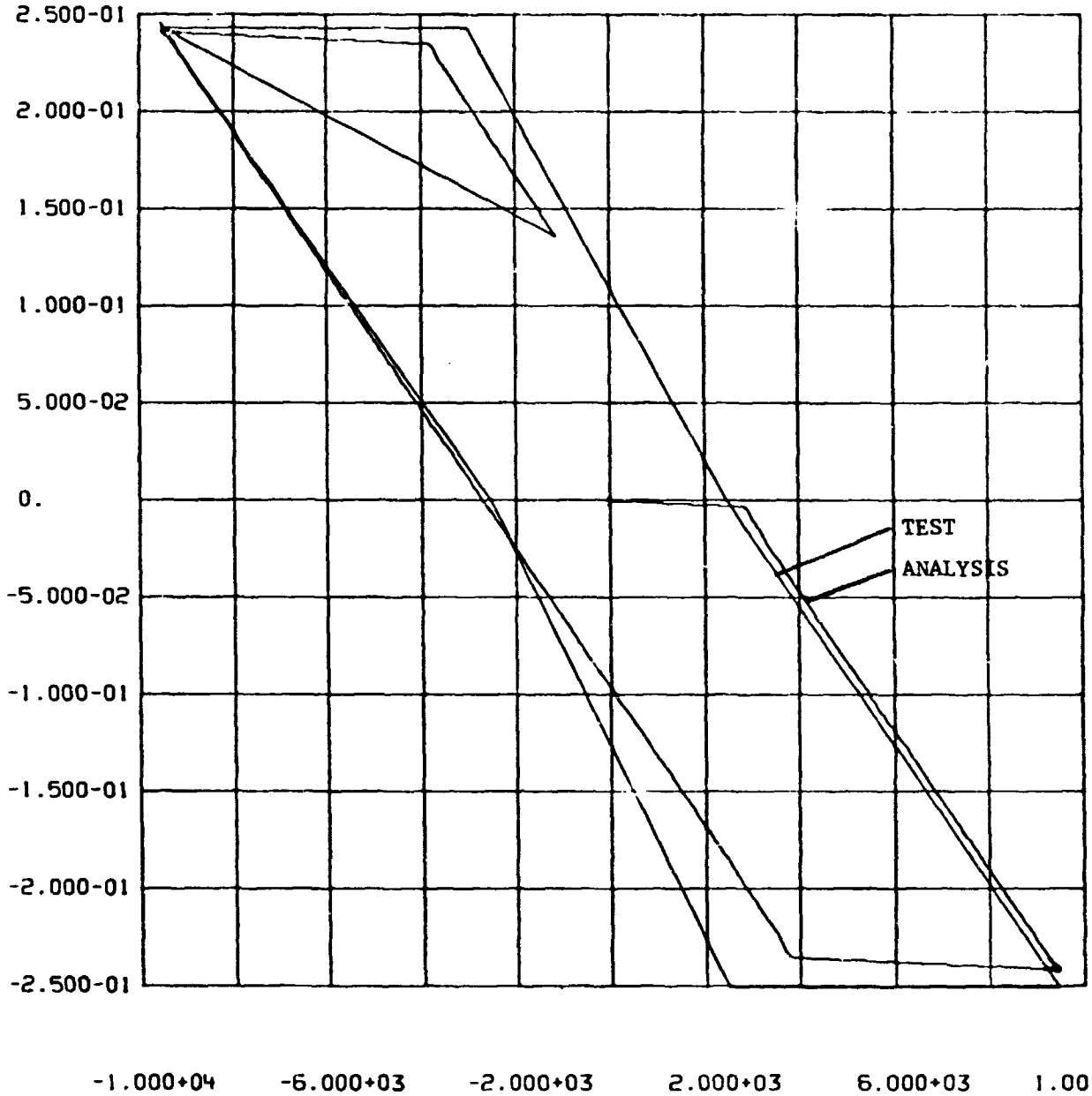

DY8 VS FORCE

1 BARLAT 20AP76 BARBER LATERAL CHECK 100K PRELOAD

FIGURE 13. ANALYSIS VERSUS TEST MEASUREMENT DY8 BARBER LATERAL TEST 100K PRELOAD

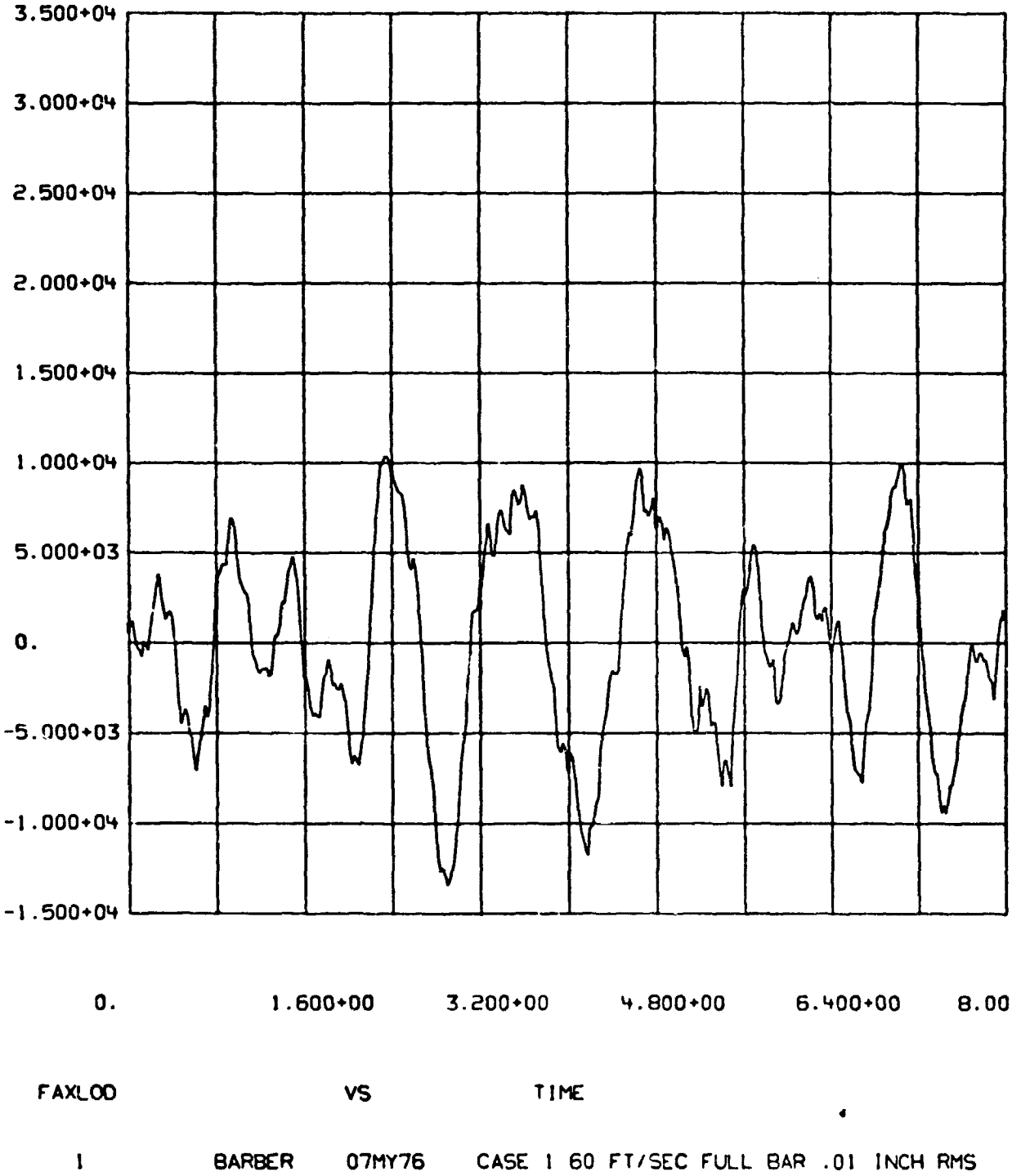

FIGURE 14. BARBER TRUCK FRONT ANLE LOAD FULL CONDITION 60 FT/SEC

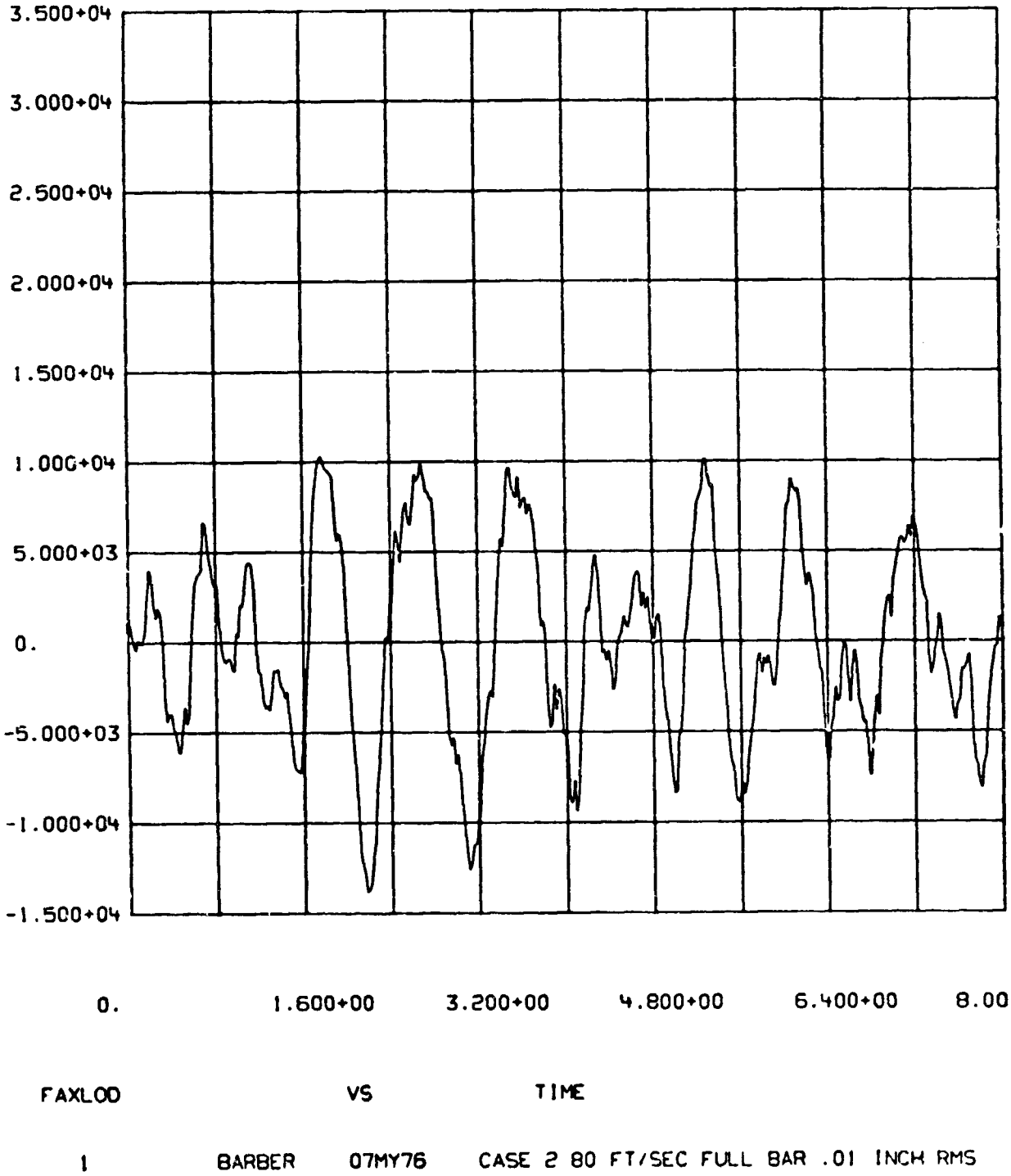

FIGURE 15. BARBER TRUCK FRONT AXLE LOAD FULL CONDITION 80 FT/SEC

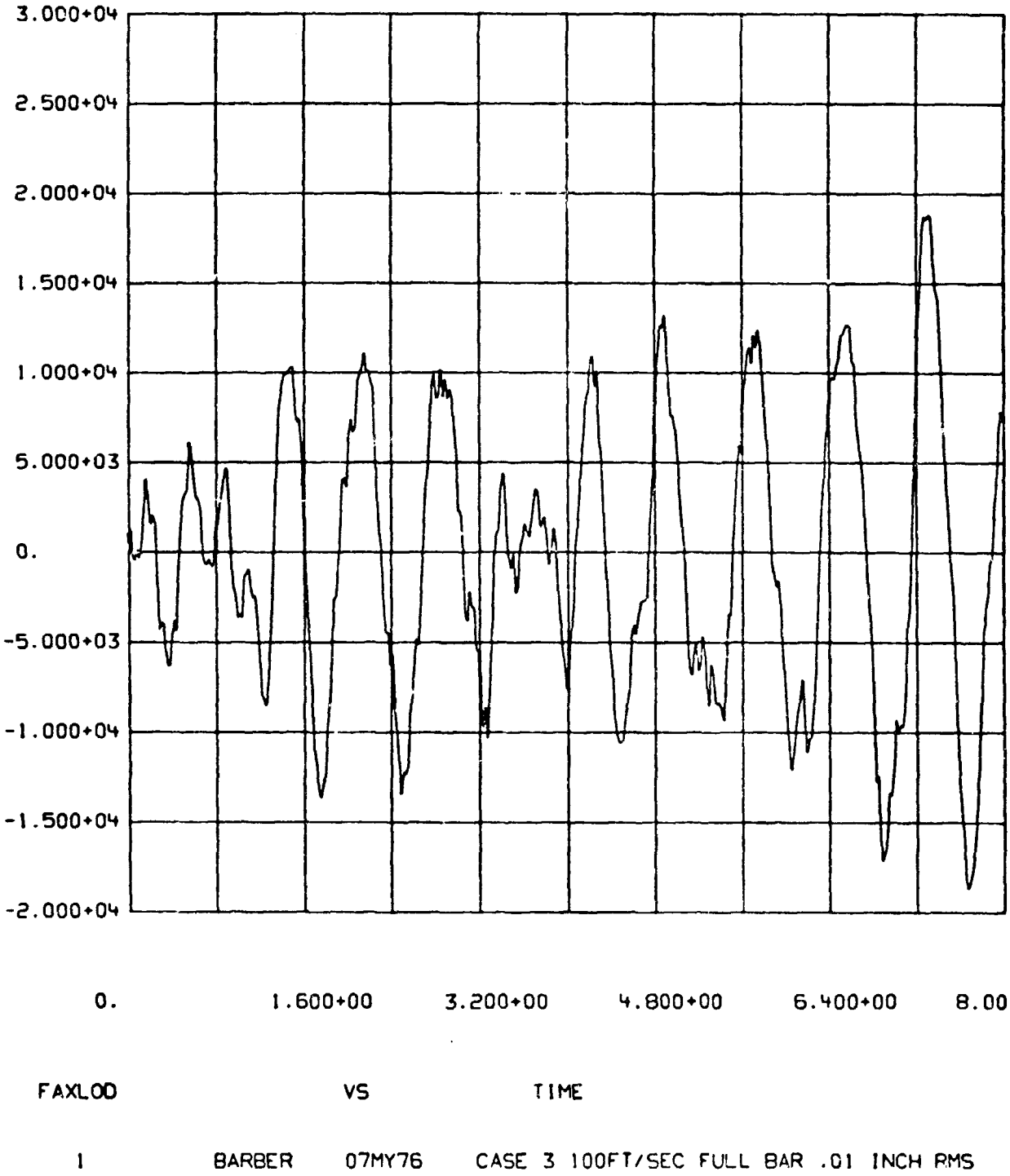

FIGURE 16. BARBER TRUCK FRONT AXLE LOAD FULL CONDITION 100 FT/SEC

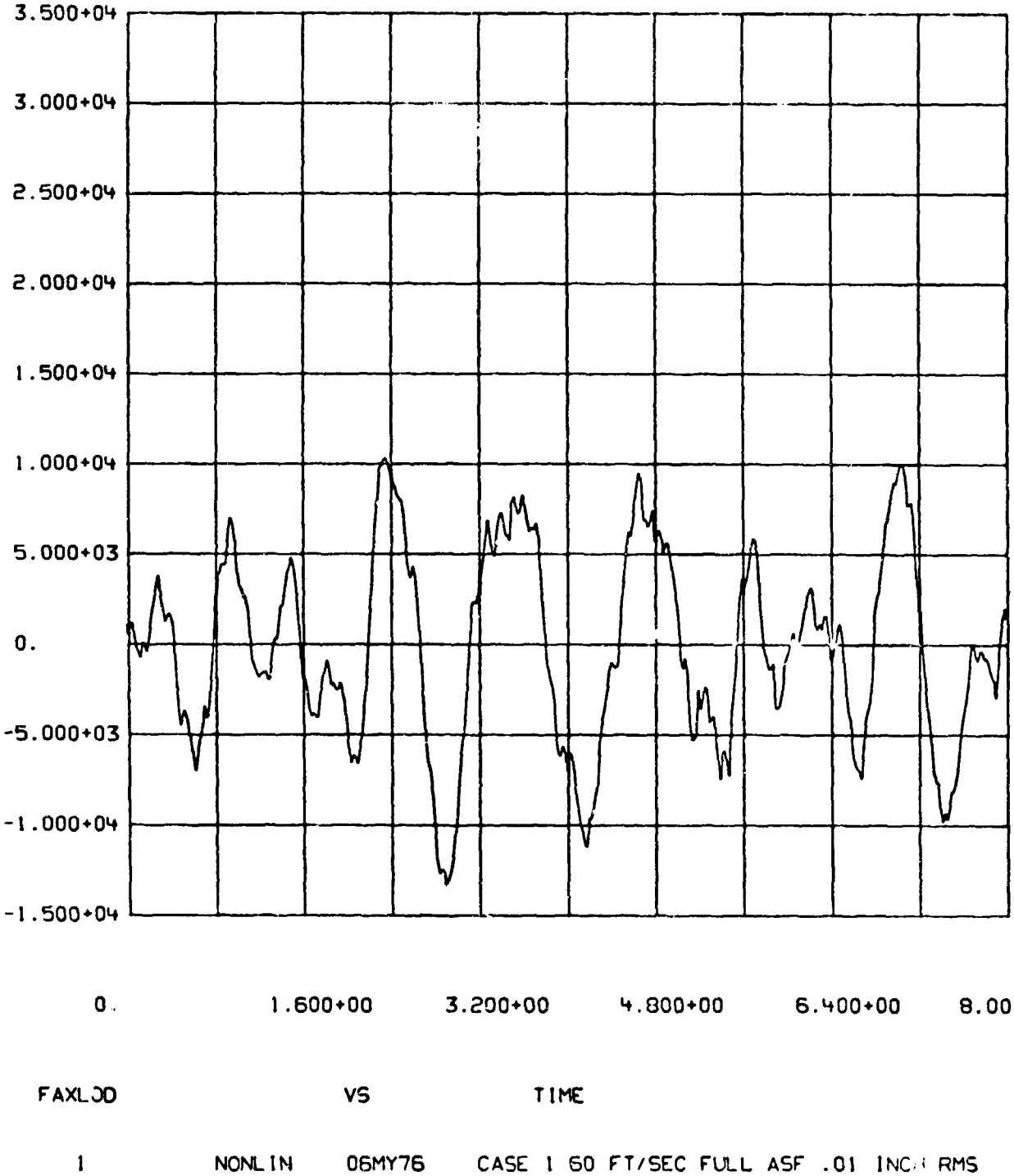

FIGURE 17. ASF TRUCK FRONT AXLE LOAD FULL CONDITION 60 FT/SEC

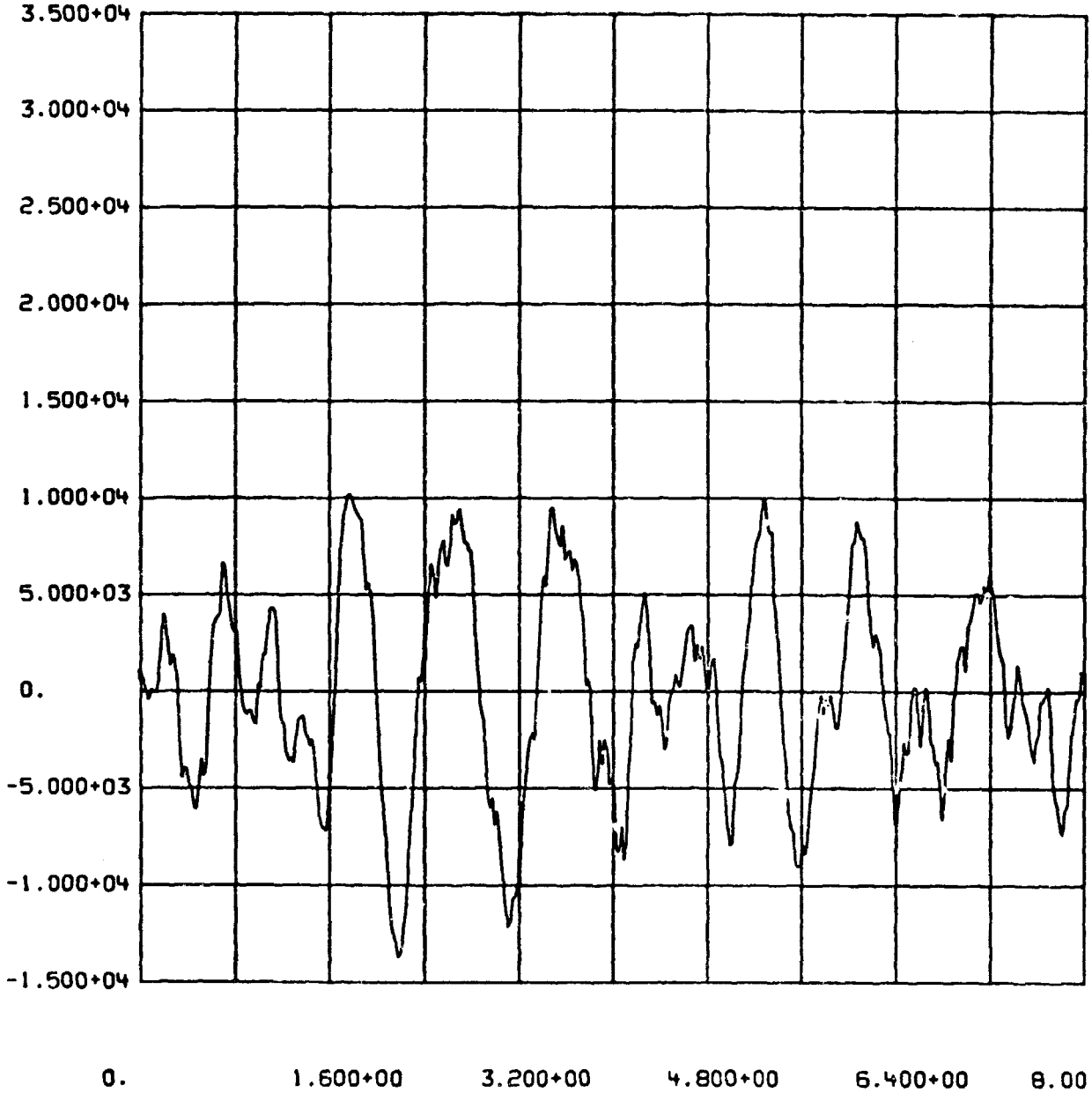

FAXLOD VS TIME

1 NONLIN 06M/76 CASE 2 80 FT/SEC FULL ASF .01 INCH RMS

FIGURE 18. ASF TRUCK FRONT AXLE LOAD FULL CONDITION 80 FT/SEC

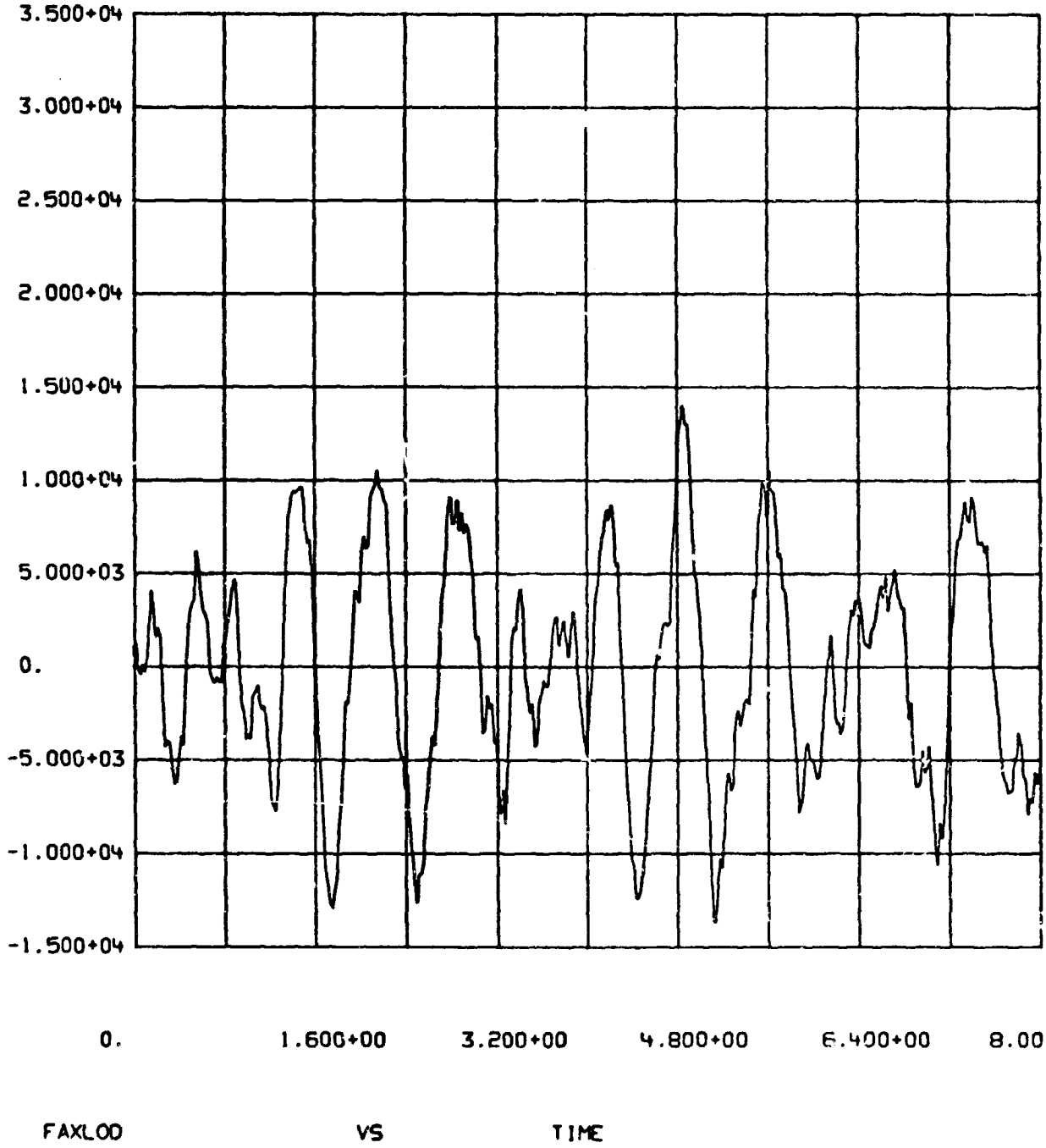

FIGURE 19. ASF TRUCK FRONT AXLE LOAD FULL CONDITION 100FT/SEC

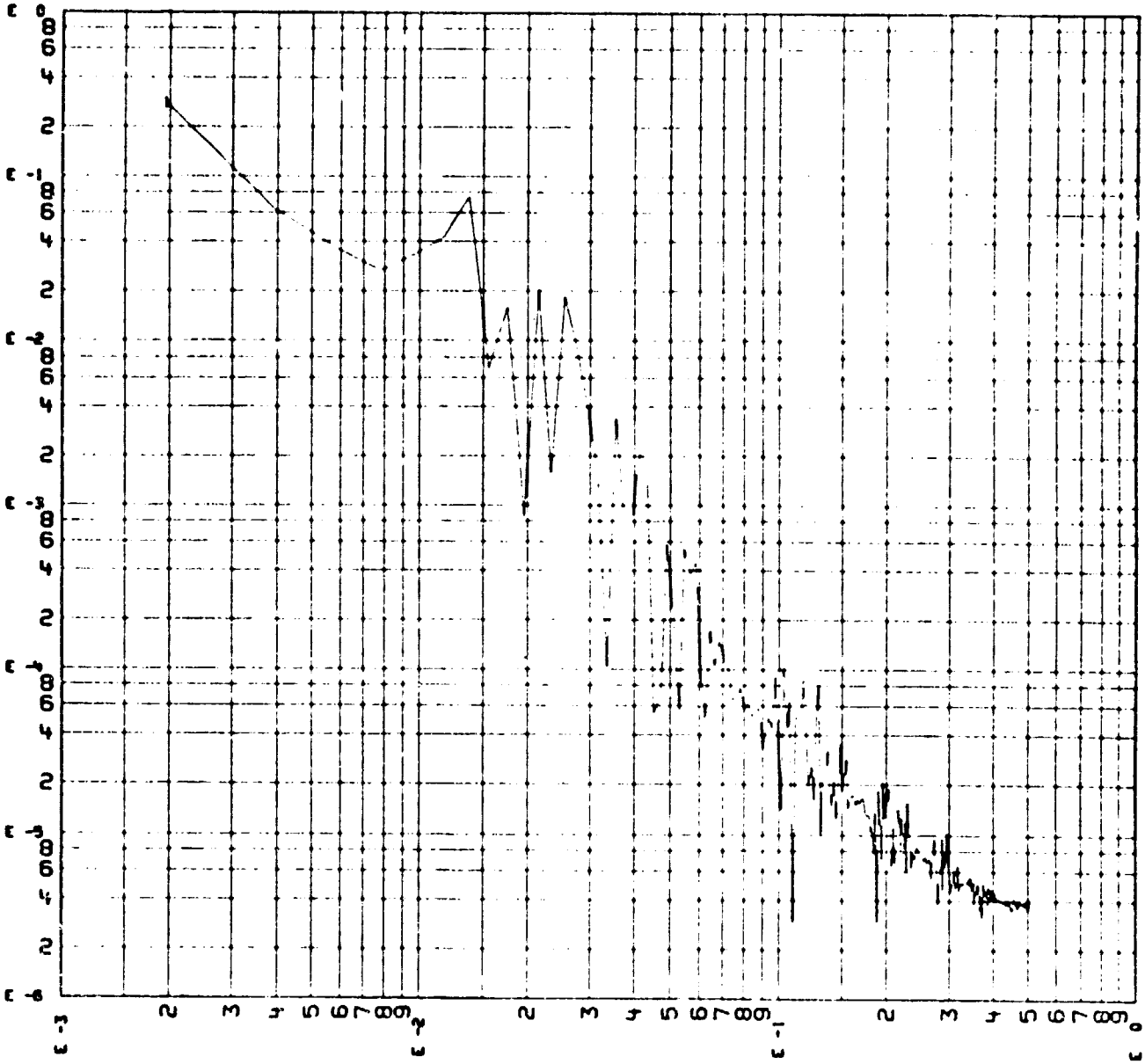

PSD VS SPATFQ

IN^2/CYCLE/FT CYCLE/FT

CHECK 09SE76 PSD OF LOW PASSED MISALINEMENT DATA

FIGURE 20. RAIL MISALINEMENT SPECTRAL DENSITY

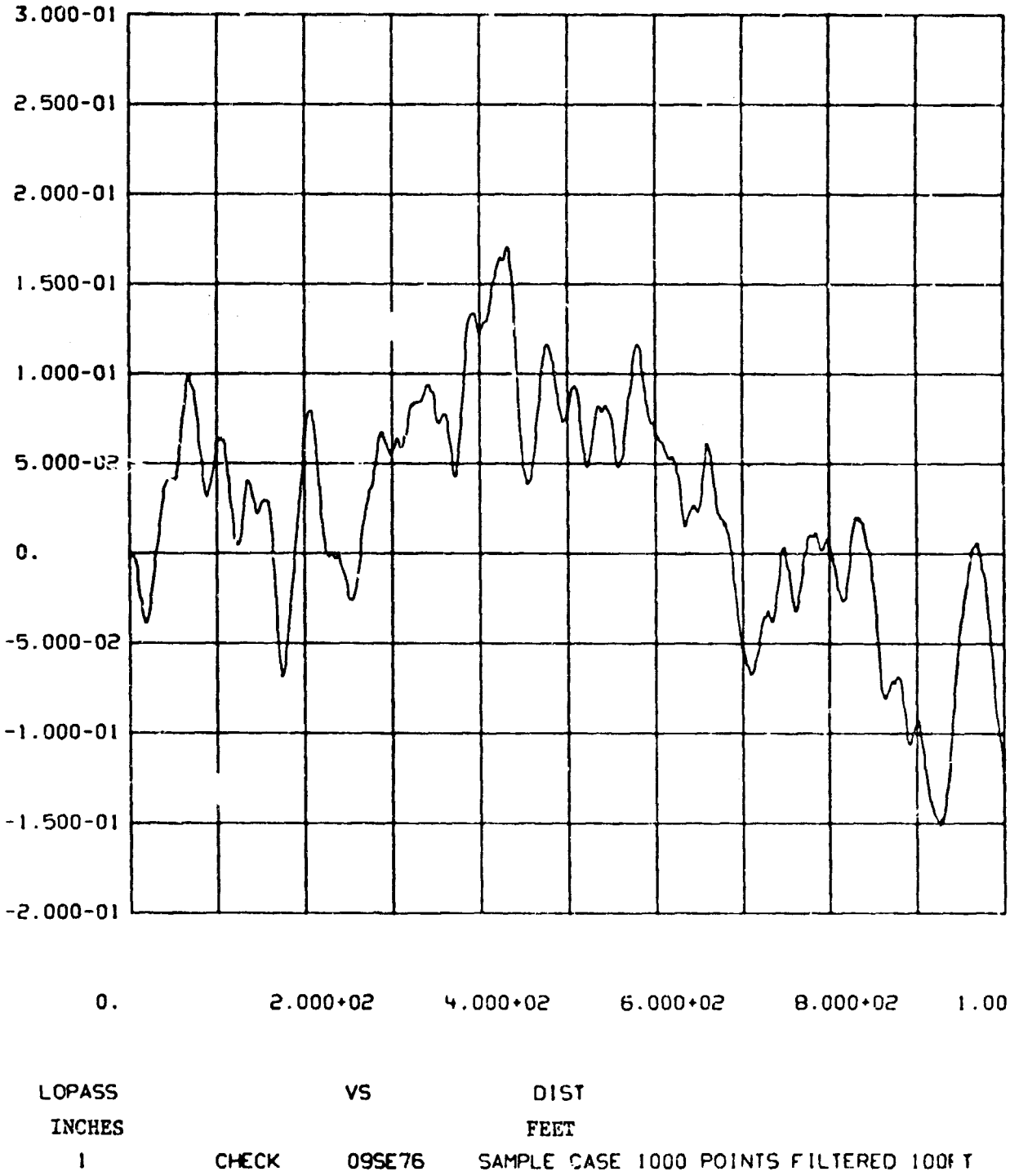

FIGURE 21. RAIL MISALINEMENT SPATIAL DISTRIBUTION

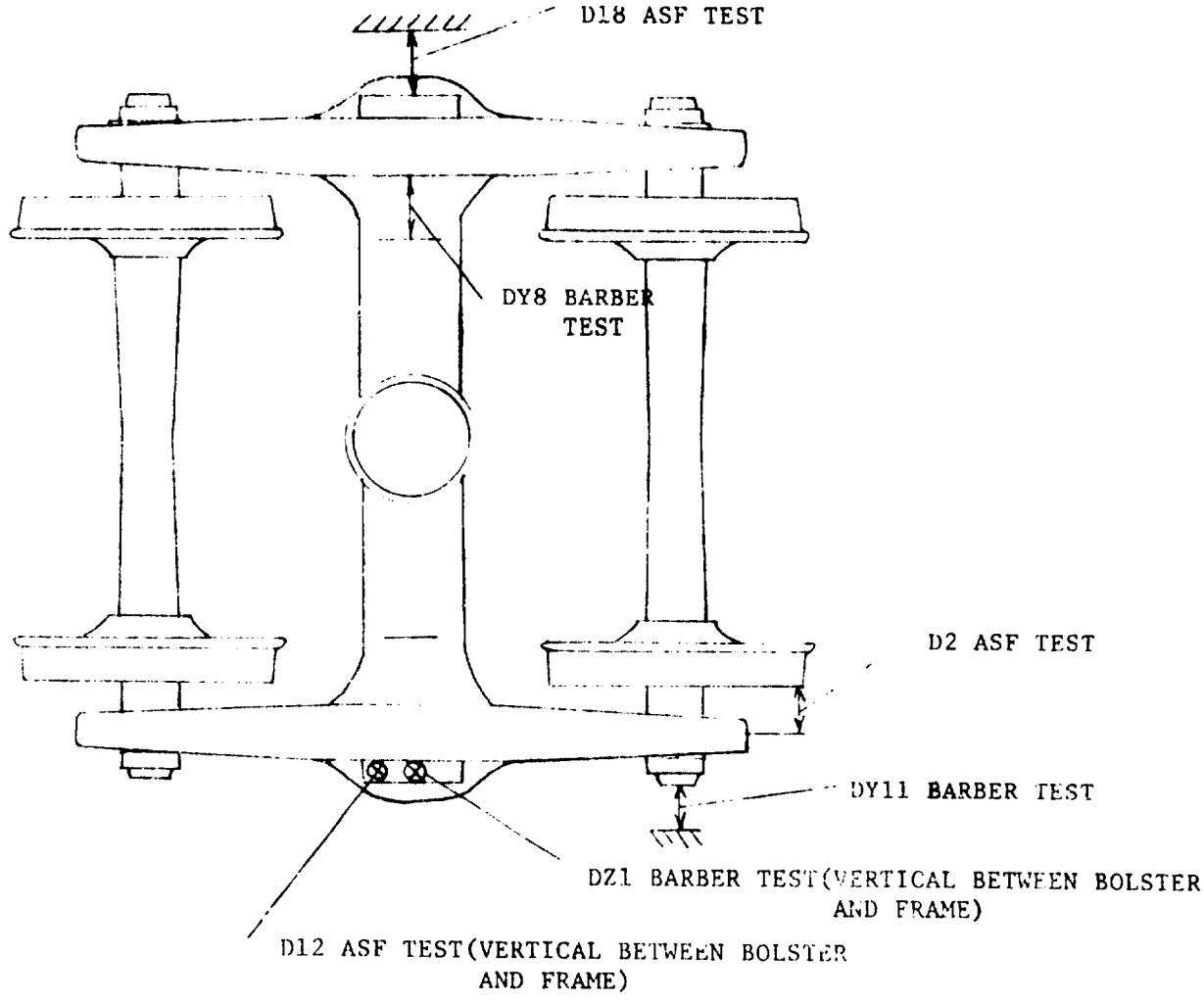

FIGURE 22. INSTRUMENT LOCATIONS